American Society for Neurochemistry

ASN Neuro
Volume 15: 1–19

DOI: 10.1177/17590914231197527
journals.sagepub.com/home/asn
Sage

SOD1^{G93A} Astrocyte-Derived Extracellular Vesicles Induce Motor Neuron Death by a miRNA-155-5p-Mediated Mechanism

Soledad Marton[1], Ernesto Miquel[1], Joaquín Acosta-Rodríguez[1], Santiago Fontenla[2], Gabriela Libisch[3], and Patricia Cassina[1]

Abstract

Amyotrophic lateral sclerosis (ALS) is a fatal neurodegenerative disease characterized by upper and lower motor neuron (MN) degeneration. Astrocytes surrounding MNs are known to modulate ALS progression. When cocultured with astrocytes overexpressing the ALS-linked mutant Cu/Zn superoxide dismutase (SOD1^{G93A}) or when cultured with conditioned medium from SOD1^{G93A} astrocytes, MN survival is reduced. The exact mechanism of this neurotoxic effect is unknown. Astrocytes secrete extracellular vesicles (EVs) that transport protein, mRNA, and microRNA species from one cell to another. The size and protein markers characteristic of exosomes were observed in the EVs obtained from cultured astrocytes, indicating their abundance in exosomes. Here, we analyzed the microRNA content of the exosomes derived from SOD1^{G93A} astrocytes and evaluated their role in MN survival. Purified MNs exposed to SOD1^{G93A} astrocyte-derived exosomes showed reduced survival and neurite length compared to those exposed to exosomes derived from non-transgenic (non-Tg) astrocytes. Analysis of the miRNA content of the exosomes revealed that miR-155-5p and miR-582-3p are differentially expressed in SOD1^{G93A} exosomes compared with exosomes from non-Tg astrocytes. Kyoto Encyclopedia of Genes and Genomes (KEGG) analysis indicates that miR-155-5p and miR-582-3p predicted targets are enriched in the neurotrophin signaling pathway. Importantly, when levels of miR-155-5p were reduced by incubation with a specific antagomir, SOD1^{G93A} exosomes did not affect MN survival or neurite length. These results demonstrate that SOD1^{G93A}-derived exosomes are sufficient to induce MN death, and miRNA-155-5p contributes to this effect. miRNA-155-5p may offer a new therapeutic target to modulate disease progression in ALS.

Keywords

ALS, astrocytes, exosomes, microRNA, miR-155-5p, motor neuron

Received September 8, 2022; Revised July 28, 2023; Accepted for publication August 9, 2023

Introduction

Amyotrophic lateral sclerosis (ALS) is a neurodegenerative condition that selectively damages the motor neurons (MNs) in the cortex, brainstem, and spinal cord (Brown & Al-Chalabi, 2017). This induces progressive paralysis that leads to death within 3–5 years postdiagnosis due to respiratory failure (Brown & Al-Chalabi, 2017). Most ALS cases are sporadic, but 5–10% have a familiar history and mendelian inheritance with more than 13 associated genes, including Cu/Zn superoxide dismutase (SOD1), TAR DNA binding protein-43 (TDP-43), fused in sarcoma (FUS), and chromosome 9 open reading frame 72 (C9Orf72), (Kiernan et al., 2011). Overexpression of mutant human SOD1 gene in rodents leads to progressive MN degeneration resembling many aspects of ALS in human patients and has contributed to elucidating various aspects of ALS pathogenesis (Gurney et al., 1994; Howland et al., 2002).

[1]Departamento de Histología y Embriología, Facultad de Medicina, Universidad de la República, Montevideo, Uruguay
[2]Departamento de Genética, Facultad de Medicina, Universidad de la República, Montevideo, Uruguay
[3]Laboratorio Hospedero Patógeno/UBM, Institut Pasteur, Montevideo, Uruguay

Corresponding Author:
Patricia Cassina, Departamento de Histología y Embriología, Facultad de Medicina, Universidad de la República, C.P. 11800, Montevideo, Uruguay.
Email: patricia.cassina@gmail.com

Although ALS is characterized by MN degeneration, glial cells play a key role in the development of the disease (Clement et al., 2003). Several neuroglia cell types, such as astrocytes, microglia, and oligodendrocytes, are involved in ALS progression (Barbeito et al., 2004; Ilieva et al., 2009). Experiments using mouse models with the ALS-associated human SOD1 with glycine to alanine substitution in position 93 ($SOD1^{G93A}$) transgene deleted in a specific cell type manner using the Cre-Lox system revealed that removal of mutant SOD1 in astrocytes or microglial cells significantly slowed ALS progression and extended life span in mice (Boillée et al., 2006; Wang et al., 2011a; 2009; Yamanaka et al., 2008b). Astrocytes are the most abundant glial cells in the central nervous system and have a major neurotrophic function for MNs. They release trophic factors and limit MN excitotoxicity by clearing glutamate from the synaptic cleft (Verkhratsky et al., 2019). ALS astrocytes change their gene expression pattern and adopt an activated state that contributes to the progression of the disease (Liddelow & Barres, 2017). Data obtained from our group and others using isolated astrocytes in coculture with MNs have demonstrated that astrocytes expressing SOD1 mutations reduce MN survival compared to non-transgenic (non-Tg) ones (Di Giorgio et al., 2007; Marchetto et al., 2008; Nagai et al., 2007; Vargas et al., 2004; Yamanaka et al., 2008a). In agreement with this, it was demonstrated that the addition of SOD1 astrocyte-conditioned medium to MNs cultures results in neurotoxicity (Fritz et al., 2013; Madill et al., 2017; Nagai et al., 2007). However, the agent responsible for astrocyte toxicity remains unknown.

Like other cell types, astrocytes modulate different biological processes by the secretion of extracellular vesicles (EVs) (Basso et al., 2013; Ceruti et al., 2011; Falchi et al., 2013; Hajrasouliha et al., 2013; Proia et al., 2008; Sbai et al., 2010; Taylor et al., 2007; Wang et al., 2011b). EVs include microvesicles and exosomes; while microvesicles are directly shed from the plasma membrane and have a heterogeneous size ranging from a dozen nanometers to a few micrometers, exosomes are generated by inward budding from the limiting membrane of endosomes forming the multivesicular bodies (MVB), which upon fusion with the plasma membrane cause exosome release (Raposo & Stoorvogel, 2013). An alteration in exosome astrocytic production and composition has been previously reported in ALS (Gharbi et al., 2020). In particular, astrocytes that express $SOD1^{G93A}$ show an increase in exosome release carrying SOD1 protein, which efficiently transfers mutant SOD1 to spinal neurons and induces selective MN death (Basso et al., 2013; Silverman et al., 2019).

Exosomes transport mRNA and microRNAs (miRNAs) from one cell to another (Ratajczak et al., 2006; Valadi et al., 2007). This is especially important in ALS, whereby RNA metabolism is altered and has been proposed to initiate cellular pathology (Arnold et al., 2013; Bilsland et al., 2010; Da Cruz & Cleveland, 2011; De Vos & Hafezparast, 2017; Murakami et al., 2002; Perlson et al., 2009; Rotem et al., 2017). In particular, the miRNA pathway is dysregulated in ALS and has been suggested as an interphase of stress and disease (Emde et al., 2015). miRNAs are RNAs of about 18–25 nucleotides long that act by binding to their target mRNAs resulting in translational repression and/or mRNA degradation (Ambros, 2004; Bartel, 2004). Two ALS-linked genes, FUS and TDP-43, are essential for miRNA biogenesis and pre-miRNA processing (Lagier-Tourenne et al., 2010). Mutations in these genes correlate with dysregulated RNA processing and metabolism in ALS cells or tissues (Le Gall et al., 2020). miRNA dysregulation has been implicated in the disease, with numerous studies supporting a role for miRNAs in ALS (Campos-Melo et al., 2013; De Felice et al., 2012; Emde et al., 2015; Hoye et al., 2017; Koval et al., 2013; Zhou et al., 2013).

Here, we further evaluated the contribution of the exosomes from $SOD1^{G93A}$ astrocytes conditioned media (CM) in their ability to influence MN survival and neurite integrity. In addition, we focus on the microRNA content of exosomes that may contribute to these effects.

Materials and Methods

Materials

Culture media and serum were obtained from Gibco (Thermo Fisher Scientific, Waltham, MA, USA). Unless otherwise specified, all other reagents were from Sigma Chemical Co. (Saint Louis, MO, USA).

Ethics Statement

Procedures using laboratory animals were conducted following international guidelines and were approved by the Institutional Animal Committee (Comisión honoraria de experimentación animal de la Universidad de la República http://www.chea.csic.edu.uy; CHEA), protocol no. 070153-000729-18.

Animals

Rats (*Rattus norvegicus*) were maintained in a controlled environment (12-h light-dark cycle; 20 ± 1°C), fed with *ad libitum* access to food and water, and housed in a cage with five female or male rats. Male hemizygous NTac: SD-Tg ($SOD1^{G93A}$) L26H rats (RRID: IMSR_TAC:2148) were obtained from Taconic (Hudson, NY, USA) and were mated with outbred Sprague–Dawley background. Progeny pups were genotyped with polymerase chain reaction (PCR), as previously described (Pehar et al., 2004; Vargas et al., 2006). In our colony, the onset of symptomatic disease (160–170 days), as well as lifespan (180–195 days), was considerably delayed from the original report (Howland et al., 2002).

Astrocyte Cultures

Cortical astrocyte cultures were prepared from 1-day transgenic $SOD1^{G93A}$ or nontransgenic rat pups genotyped by PCR as previously described (Pehar et al., 2004; Vargas et al., 2006). Briefly, the brain cortex was dissected, meninges were carefully removed, and tissue was chopped and dissociated with 0.25% trypsin-EDTA for 25 min at 37°C. Trypsinization was stopped with Dulbecco's modified Eagle's medium supplemented with 10% fetal bovine serum (s-DMEM) in the presence of 50 µg/ml DNase I. Subsequently, the tissue was mechanically disaggregated by repeated pipetting, and the suspension was passed through an 80-µm mesh and spun 10 min at $300 \times g$. The pellet was resuspended in s-DMEM medium and plated at a density of 1.5×10^6 cells per 25-cm^2 tissue culture flask. When confluent, cultures were shaken for 48 h at 250 rpm and incubated for another 48 h with 10 µM cytosine arabinoside. Next, cells were plated at a density of 2×10^4 cells/cm^2 in a 75 cm^2 Nunc flask (Nunc, Thermo Fisher Scientific). Astrocytes were maintained in s-DMEM, 4-(2-hydroxyethyl)-1-piperazineethanesulfonic acid (HEPES, 3.6 g/L), penicillin (100 IU/mL), and streptomycin (100 mg/mL). Astrocyte monolayers were 98% pure as determined by glial fibrillary acidic protein (GFAP) immunoreactivity.

MN Cultures

MN cultures were prepared from embryonic day 15 (E15) rat spinal cord by a combination of OptiPrep™ (Merck, Rahway, NJ USA, 1:10 in L15 medium) gradient centrifugation and immunopanning with the monoclonal antibody 192-IgG hybridoma supernatant (Chandler et al., 1984) against p75 low-affinity neurotrophin receptor as previously described with minor modifications (Henderson et al., 1993). The remaining cell population after immunopanning consisted of over 95% neurons, expressing the MN markers p75 and ISLet1. Purified MNs were seeded at a density of 300 cells/cm^2 onto confluent glial feeder layers (FL) in s-Leibovitz's L15 medium or on a polyornithine–laminin substrate and maintained in s-Neurobasal™ (NB) medium. MN cultures were supplemented with 1 ng/ml glial cell-derived neurotrophic factor (GDNF) as previously described (Cassina et al., 2002; Díaz-Amarilla et al., 2011) and subjected to different treatments described later. For RNA extraction, when high amounts of MNs were required, immunopanning was avoided.

Exosome-Enriched Fraction

Exosomes were isolated from a conditioned medium harvested from a confluent monolayer of cultured astrocytes from two 75 cm^2 flasks (6×10^6 astrocytes on 30 ml final volume). Before CM extraction, astrocytes were washed twice with phosphate-buffered saline (PBS, $NaCl_2$ 137 mM, 2.7 mM KCl, 4.3 mM $Na_2HPO_4 \cdot 7H2O$, 1.5 mM KH_2PO_4) and incubated with DMEM, supplemented with HEPES (3.6 g/L), penicillin (100 IU/ml), and streptomycin (100 mg/ml). After 24 h incubation, exosomes were prepared from astrocyte culture mediums. Exosomes were purified as described previously with minor modifications (Thery et al., 1999) by three successive centrifugations at $300 \times g$ (10 min), $2{,}000 \times g$ (10 min), and $10{,}000 \times g$ (30 min) to eliminate cells and debris followed by a $100{,}000 \times g$ centrifugation for 80 min. The exosome pellet was washed once in 6 ml PBS, centrifuged $100{,}000 \times g$ (1 h), and resuspended in 30 µl of PBS or 200 µl TRIzol® (Thermo Fisher Scientific) or protein lysis buffer for western blotting. To evaluate exosome integrity or exosome membrane protein in survival or neuron morphometric parameter experiments, fractions were subjected to incubation with 0.25% trypsin or Milli-Q water for 10 min at 37°C, as described previously (Lopez-Verrilli et al., 2013). After treatment, fractions were washed in PBS, ultracentrifuged, and resuspended in PBS. The exosomes obtained were analyzed by Microfluidic Resistive Pulse Sensing (MRPS, Spectradyne, Torrance, CA) to determine the size and concentration of the exosomes (Arab et al., 2021). A mean concentration of $12.8 \pm 6.3 \times 10^{10}$ particles/ml was obtained, corresponding to approximately 4,000 particles per astrocyte.

MNs Treatment and Counting

After being cultured for 24 h, MNs were subjected to the following treatments: astrocytic conditioned medium (CM), exosome-free astrocyte CM (at a 1:10 dilution), or exosomes at a concentration of 6.4×10^8 particles/ml. This concentration is equivalent to approximately 5×10^5 particles/MN, which matches the final concentration present in a similar volume of astrocyte CM. Additionally, MNs were treated with either a 0.01 µM 155-5p miRNA mimetic (MIMAT0030409 Ambion, Thermo Fisher Scientific) or an inhibitor (MIMAT0030409, Ambion, Thermo Fisher Scientific).

After 24–48 h posttreatment, cells were processed for immunofluorescence and MN counting. MN survival was assessed by directly counting all intact neurites longer than 4 somas in diameter in a prefixed area of the dishes. Counts were performed in an area of 0.90 cm^2 along a diagonal in 24-well plates.

Western Blot Analysis

Proteins were extracted from exosomes enriched fraction in 1% SDS supplemented with 2 mM sodium orthovanadate and a complete protease inhibitor cocktail (Roche, Basel, Switzerland). Lysates were resolved by electrophoresis on 12% SDS–polyacrylamide gels and transferred to a polyvinylidene fluoride membrane (PVDF; Thermo Fisher Scientific).

The membrane was blocked for 1 h at room temperature in 5% skimmed milk in TBS-T (Tris-buffered saline with 0.1% Tween). The membrane was then probed overnight with primary antibodies in 1% skimmed milk in TBS-T at 4°C. Primary antibodies include rabbit monoclonal anti-TSG101, 1:1,000 (Abcam, Cambridge, UK, Cat# ab125011, RRID: AB_10974262); mouse monoclonal anti-flotillin-1, 1:500 (BD Biosciences, Franklin Lakes, NJ, USA, Cat# 610820, RRID: AB_398139); rabbit polyclonal anti-human SOD1 antibody kindly provided by Prof. Mónica Marin from Facultad de Ciencias, UdelaR, 1:500 (Palacios et al., 2010); and rabbit polyclonal anti-BIP, 1:1,000 (Abcam, ab21685, RRID: AB_2119834). Afterward, the membranes were washed in TBS-T and incubated for 60 min at room temperature with IRDye 680RD-conjugated goat anti-mouse IgG and IRDye 800CW-conjugated goat anti-rabbit IgG secondary antibodies (1:15,000 in PBS each, LI-COR Biosciences, Cat# 926-68070, RRID: AB_10956588 and Cat# 925-68071, RRID: AB_2721181, respectively). The Odyssey system (LI-COR Biosciences) was used to detect the bands.

Electron Microscopy

Exosomes were processed for transmission electron microscopy (TEM) by negative staining with 2% uranyl acetate at the Electron Microscopy Unit (Facultad de Ciencias, Universidad de la República, Montevideo, Uruguay). Briefly, astrocyte exosome-enriched fractions were prepared as mentioned and resuspended in 30 µl PBS. 10 µl exosome suspension was added on top of carbon film-coated electron microscopy grids (Electron Microscopy Sciences) and incubated for 15 min, and excess liquid was removed with filter paper. Samples were incubated with 2% uranyl acetate for 5 min, with excess liquid removed as before, and let dry completely before imaging. Exosome preparations were examined using a Jeol JEM1010 TEM operated at 100 kV and equipped with 4,000 AM DVC and a HAMAMATSU C-4742-95 digital camera under the control software AMT ADVANTAGE. The exosome diameter was measured in electron micrographs using Fiji (ImageJ) software (NIH; RRID: SCR_002285).

Immunofluorescence

MN cultures were fixed for 15 min on ice with 4% paraformaldehyde plus 0.1% glutaraldehyde in PBS. The cultures were permeabilized with 0.1% Triton X-100 for 15 min and incubated for 2 h at room temperature (25°C) in blocking solution [0.1% Triton X-100, 2% bovine serum albumin (BSA), and 10% goat serum in PBS]. Primary antibodies diluted in the blocking solution were incubated overnight at 4°C. After washing with PBS, the cultures were further incubated for 1 h at room temperature with the secondary antibodies diluted in the blocking solution. The slides were then washed with PBS, rinsed with distilled water, and mounted with Prolong Antifade mounting kit (Thermo Fisher Scientific). The primary antibody used was mouse anti-beta III tubulin (1:3,000, Abcam, Cambridge, UK, Cat# ab41489, RRID: AB_727049), and the secondary was Alexa Fluor 488-conjugated goat anti-mouse IgG secondary antibody (1:1,000, Thermo Fisher Scientific, # A-11029, RRID: AB_2534088). Nuclei were stained with DAPI. Images were captured with a DC290 Zoom Kodak Digital Camera coupled to a Nikon fluorescence microscope.

RNA Extraction and Quantitative RT-PCR

Astrocyte cells and exosomes were lysed with TRIzol reagent (Thermo Fisher Scientific, USA) to extract the required RNA, as the manufacturer's instructions recommended. To increase the RNA yields, minor modifications were applied at the precipitation step of exosome RNA purification. Briefly, RNA precipitation was performed with two volumes of isopropyl alcohol; 5 µg linear acrylamide was added, and the solution was incubated for 20 min at −20°C. After 30 min centrifugation at 12,000*g*, 4°C supernatant was discarded, and RNA was resuspended in 20 µl nuclease-free water (Thermo Fisher Scientific) and 40 U RNase inhibitor (Thermo Fisher Scientific). Possible DNA contaminations were eliminated with DNase treatment using the DNase-free Kit (Thermo Fisher Scientific). RNA quality was evaluated by agarose gel electrophoresis followed by ethidium bromide staining or by using Agilent 2100 BioAnalyzer (Agilent, Santa Clara, CA, USA). RNA quantification was performed by 260 nm absorption using a nanodrop spectrophotometer (Thermo Fisher Scientific).

Mature miRNA qPCR was done by Stem Loop RT-qPCR as described previously (Kramer, 2011) and mRNA by SYBR Green-based RT-qPCR. Briefly, before starting Stem Loop RT-qPCR, a stock solution of 100 µM SL primer was done and after was folded by heating to 95°C for 10 min. Heat was slowly reduced to 75°C, and then, the temperature was held at 75, 68, 65, and 62°C for an hour each and held at 60°C for 4 h, and the solution was stored at −20°C. Stem Loop RT-qPCR was done by reverse transcription of 5 ng of total RNA with 1 µl SL primer (1 µM), 0.5 µl dNTPs (10 µM), 5xRT buffer, 2 µl DTT, and 1 µl M-MLV-reverse transcriptase 200 U/µl (Thermo Fisher Scientific) in a final volume of 20 µl. Retrotranscription was done in a thermal cycler by incubation for 30 min at 16°C, followed by pulsed RT of 60 cycles at 30°C for 30 s, 42°C for 30 s, and 50°C for 1 s. After that, the reaction was incubated at 85°C for 5 min. For real-time PCR, 1 µl of the cDNA was used in Biotools Quantimix Easy master mix (Biotools, South San Francisco, CA, USA) with 0.5 µl primer mix (Universal RV and Fw miR specific primers, Fw:Rev, 5 µM:1 µM) in a final volume of 10 µl. Samples were incubated at 95°C for 10 min, followed by cycles of 95°C for 15 s, 60°C for 20 s, and 92°C for 0.5 seg using a Rotor-Gene 6000 System

(Corbett, Life Science), and data were analyzed using Rotor-Gene 6000 software (Corbett Life Science; RRID: SCR_017552). The ΔΔCt method was performed using MNs without treatment with exosomes as a negative control and GAPDH mRNA as an exogenous reference control.

For conventional real-time PCR, 100 ng of this total RNA was reverse transcribed using the MLV-reverse transcriptase, 200 U/µl, and 1 µl of the resulting cDNA was diluted in Biotools Quantimix Easy master mix and amplified by PCR over 40 cycles using the Corbett System. Collected data were analyzed using Rotor-Gene software. The ΔΔCt method was performed using MNs without treatment with exosomes as a negative control and GAPDH mRNA as an exogenous reference control. GAPDH was used as an endogenous reference gene because of its well-documented stability and its prior utilization in exosomal miRNA studies (Chen et al., 2022; Gorji-Bahri et al., 2021; Shi et al., 2015; Yu et al., 2020). Moreover, PCR analysis confirmed the presence of GAPDH mRNA in every sample, providing additional evidence to support its suitability as a normalization control.

All reactions were done in 10 µl volume and triplicate in strip tubes (Axygen® Brand Products, San Francisco, CA, USA), using specific forward and reverse primers (Table 1).

In all cases, a uniform amplification of the products was rechecked by analyzing the melting curves of the amplified products (dissociation graphs), and gel electrophoresis was performed to confirm the correct size of the amplification and the absence of nonspecific bands.

To predict messengers targeted by miR-155-5p or miR-582-3p, we used TargetScan (Agarwal et al., 2015) and DIANA-microT-CDS (Paraskevopoulou et al., 2013; Vlachos et al., 2015). Because we wished to extrapolate our results to humans for its greater accuracy than *Rattus norvegicus,* we used the *Homo sapiens* database to predict miRNA target genes. miRNAs predicted targets that were predicted with both algorithms were used in an enrichment analysis with DAVIDv6.8 (Huang et al., 2009; Sherman et al., 2022) online software to identify overrepresented Kyoto Encyclopedia of Genes and Genomes (KEGG) signaling pathways and Gene Ontology (GO) categories (biological process, molecular function, and cellular component). The terms with modified Fisher exact *p*-value (EASE score) $\leq .05$ and false discovery rate (FDR) ≤ 0.05 were considered significantly enriched.

Statistics

All culture assays were performed in duplicate, and each experiment was repeated at least three times. Quantitative data were expressed as mean ± standard error of the mean (SEM). Paired one- or two-tailed *t*-tests were performed to compare data with two experimental groups. A two-way analysis of variance (ANOVA) followed by Fisher's LSD test for multiple comparisons or a one-way ANOVA followed by Tukey's multiple comparisons test was performed as indicated using GraphPad Prism version 8.0.0 for Windows, GraphPad Software, San Diego, CA, USA. A value of $p \leq .05$ was considered statistically significant.

Results

Exosomes are Obtained From Astrocyte CM

After successive centrifugations of CM from astrocyte primary cultures, we obtained a pellet fraction from 100,000 × *g* ultracentrifugation (p100). This fraction was analyzed by TEM following negative staining. The micrographs showed several arrays of round-shaped vesicles. Around 77% of the total vesicles measured were between 60 and 100 nm in diameter with a median of 100.2 nm, which is in the range reported for exosome size (Raposo & Stoorvogel, 2013) (Figure 1(a) and (b)). To further characterize this fraction, the presence of the exosome-specific proteins flotillin-1 (Thery et al., 1999) and the component of the endosomal sorting complex responsible for transport 1 (ESCRT-I): tumor susceptibility gene 1 (TSG101) (De Gassart et al., 2003) were assayed by western blotting. Flotillin-1 and TSG101 were detected in all p100 fractions analyzed (Figure 1(c)). Moreover, the exosomes were negative for BiP, which is a protein found in the endoplasmic reticulum (Supplemental Figure 1). These findings suggest that the samples are enriched in exosomes and do not contain other subcellular components. In addition, the presence of the human SOD1 was analyzed in the same fraction as had been previously shown (Basso et al., 2013). As expected, human SOD1 was present exclusively in $SOD1^{G93A}$ – but not in the non-Tg-derived exosomes.

SOD1^{G93A} Astrocytes-Derived Exosomes Exhibit the Characteristic RNA Size Profile and No Detectable Levels of Human *SOD1*^{G93A} mRNA

Previous reports indicate that exosomes contain substantial amounts of RNA (Valadi et al., 2007). The electropherogram profile of total RNA from the astrocyte-derived exosomes was compared to the total RNA extracted from cultured astrocytes and analyzed (Figure 2(a)). As described, the RNA extracted from exosomes included a broad range of RNA sizes (30–500 nt), with undetectable levels of 18S and 28S ribosomal RNAs (rRNAs). However, these ribosomal RNAs were present in RNA extracted from cultured astrocytes. The presence of human SOD1 (hSOD1) mRNA in exosomes of $SOD1^{G93A}$ astrocytes was analyzed by RT-PCR. Although $SOD1^{G93A}$ protein was detected in the exosomes of $SOD1^{G93A}$ astrocytes, hSOD1 mRNA was not identified in any of the analyzed samples (Figure 2(b)).

Table 1. List of Primer Sequences of Primers Employed for Real-Time RT-PCR.

Name	Sequence
GFAP	5′-CACTGAGCATCTCCCTCACAA-3′
	5′-TGGTATTCGAGAGAAGGGAGG-3′
SOD1	5′-CACCAGTGTGCGGCCAATGA-3′
	5′-GTGGCATCAGCCCTAATCCA-3′
GAPDH	5′-CACTGAGCATCTCCCTCACAA-3′
	5′-TGGTATTCGAGAGAAGGGAGG-3′
Universal RV primer	5′-CCAGTGCAGGGTCCGAGGTA-3′
miR-9-5p	5′-GTCGTATCCAGTGCAGGGTCCGAGGTATTCGCACTGGATACGACTCATAC-3′
	5′-GCGGCGGTCTTTGGTTATCTAGC-3′
miR-23a	5′-GTCGTATCCAGTGCAGGGTCCGAGGTATTCGCACTGGATACGACGGAAAT-3′
	5′-CGGCGGATCACATTGCCA-3′
miR-124-3p	5′-GTCGTATCCAGTGCAGGGTCCGAGGTATTCGCACTGGATACGACGGCATT-3′
	5′-CACGCATAAGGCACGCGG-3′
miR-132-3p	5′-GTCGTATCCAGTGCAGGGTCCGAGGTATTCGCACTGGATACGACCGACCA-3′
	5′-GCGGCGGTAACAGTCTACAGC-3′
miR-155-5p	5′-GTCGTATCCAGTGCAGGGTCCGAGGTATTCGCACTGGATACGACACCCCT-3′
	5′-GCGGCGGTTAATGCTAATTGTGAT-3′
miR-582-3p	5′-GTCGTATCCAGTGCAGGGTCCGAGGTATTCGCACTGGATACGACGGGTTC-3′
	5′-GCGGCGGAACCTGTTGAAC-3′

miR-155-5p and miR-582-3p in silico target prediction.

SOD1^{G93A} Astrocyte-Derived Exosomes are Sufficient to Reduce the Survival of MNs and the Length of Neurites

To address the role of SOD1^{G93A} astrocyte-derived exosomes on the ability of astrocytes to promote the survival of MNs, we compared the effects of non-Tg or SOD1^{G93A} astrocytes CM versus exosomes on purified non-Tg MN cultures exposed to GDNF (Figure 3). CM from SOD1^{G93A} astrocytes (1:10 dilution) significantly reduced the survival of MNs exposed to GDNF, compared to CM from non-Tg astrocytes, as previously reported (Figure 3(a) and (b)) (Fritz et al., 2013; Madill et al., 2017; Nagai et al., 2007). The incubation of pure MN cultures with SOD1^{G93A} astrocyte exosomes induced a significant reduction in MN survival in the presence of GDNF ($25.6\% \pm 10.6$), while no such effect was detected when non-Tg exosomes were applied to MN cultures (Figure 3(a) and (b)). The reduced ability of SOD1^{G93A} astrocyte CM to support MN survival was not present when EVs were depleted from SOD1^{G93A} astrocytes CM (Figure 3(b)).

In addition, the effect of the exosomes on the length and branching of MN neurites was assessed. Neurite length was significantly decreased in MNs treated with SOD1^{G93A} astrocyte-derived exosomes compared to non-Tg ones following GDNF exposure (Figure 3(c) and (d)). There was a $21 \pm 12\%$ and a $22 \pm 6\%$ decrease in the longest neurite (Figure 3(c)) and total neurite length (Figure 3(d)), respectively. The morphology of motoneuron arborizations, as revealed by the Sholl analysis, is characterized by few neurites emerging from the soma and usually the longer one branches near the end. The length of the longest neurite varies among cells. Neurite branching showed an overall reduced complexity in MNs treated with exosomes from SOD1^{G93A} astrocytes significant at 150 μm from the soma (Figure 3(e)). SOD1^{G93A} astrocyte exosome-mediated effects were abolished when exosome membrane integrity was disrupted or membrane proteins were digested. MNs incubated with exosome preparations that were subjected to osmotic shock or trypsin digestion induced no significant changes in the longest neurite or total neurite length (data not shown).

miR-155-5p and miR-582-3p are Dysregulated in SOD1^{G93A} Astrocyte Exosomes

Because exosomes can transport miRNAs that are functionally transferred to other cells (Lopez-Verrilli et al., 2013; Record et al., 2014) and miRNA profile is altered in ALS, we assessed whether miRNAs that have been reported to show modified expression in ALS (Paez-Colasante et al., 2015) were differentially expressed in SOD1^{G93A} astrocyte exosomes (Table 2).

Most of the analyzed miRNAs were expressed in cultured whole astrocytes, but only miR-155-5p and miR-582-3p were also detected in the exosomes (Table 2). Notably, there were significant differences in the gene expression levels of miR-155-5p and miR-582-3p between SOD1G93A astrocyte exosomes and non-Tg exosomes (Figure 4). Specifically, miR-155-5p was upregulated, while miR-582-3p was downregulated in SOD1G93A astrocyte exosomes (Figure 4(b) and (d)). Interestingly, the expression levels of miR-155-5p

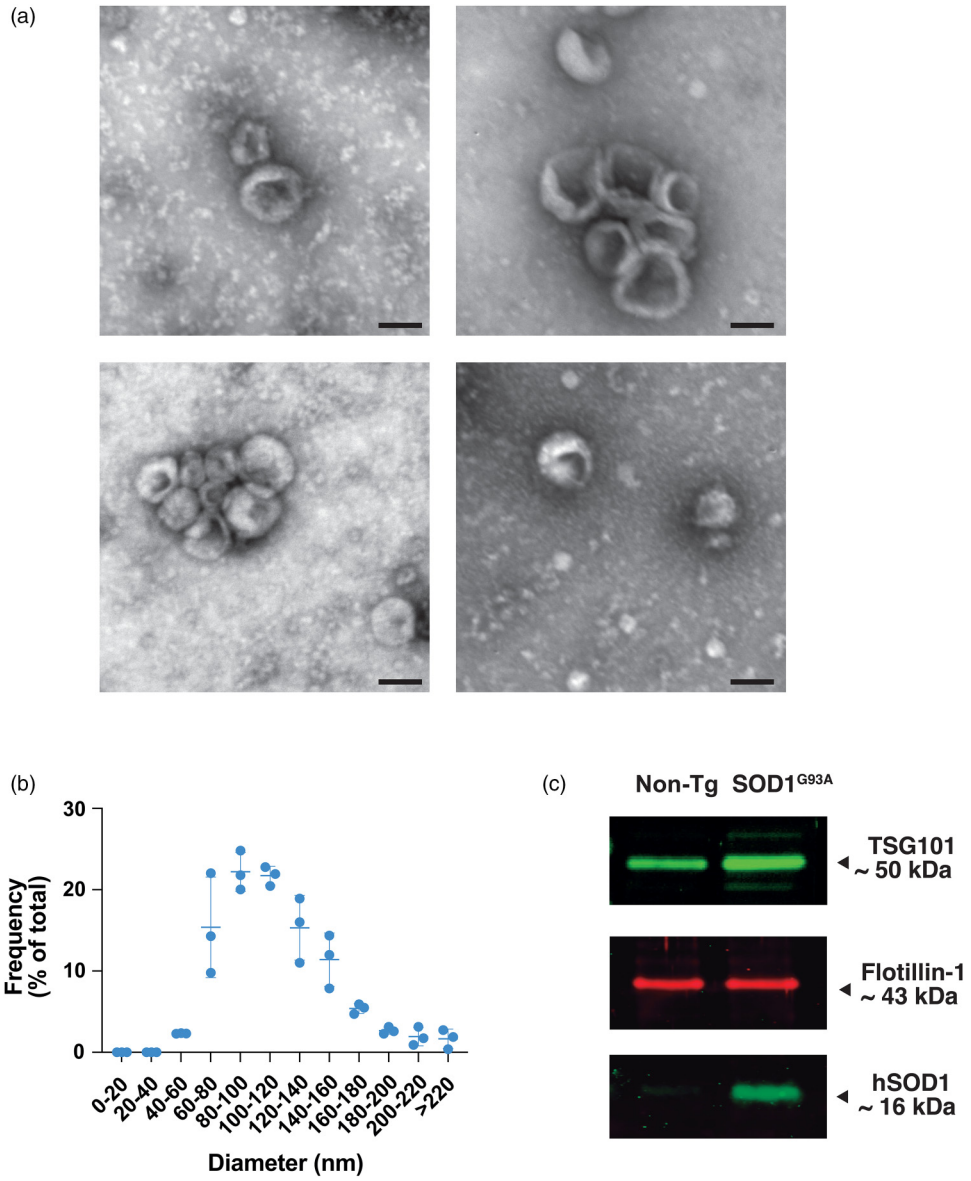

Figure 1. Morphological characterization and size distribution of extracellular vesicles present in astrocyte CM. (a) TEM micrographs (negative staining) from extracellular vesicles isolated from astrocyte CM. Bars: 100 nm. (b) Frequency distribution of EV diameter as a percentage of the total number of vesicles from the three independent experiments. (c) Representative western blot of the exosomes from non-Tg or SOD1^{G93A} astrocyte CM using antibodies against TSG101, flotillin-1, and human SOD1.

were significantly lower in whole SOD1^{G93A} astrocytes than in non-Tg ones (Figure 4(a)).

KEGG Analysis Shows That miR-155-5p and miR-582-3p Predicted Targets are Enriched in Neurotrophin Signaling Pathway Genes

To gain insights into miR-155-5p and miR-582-3p miRNA regulatory mechanisms, we searched for potential gene targets and associated signaling pathways using TargetScan (Agarwal et al., 2015) and DIANA-microT-CDS (Paraskevopoulou et al., 2013; Vlachos et al., 2015) bioinformatic platforms (Figure 5).

For miR-155-5p, 556 predicted target genes were found with TargetScan and 1,082 with DIANA-T-CDS. In total, 345 targets were predicted at the intersection of both algorithms (Figure 5(a)). Out of these, 341 were identified in the DAVID database and used in GO enrichment analyses (Figure 5(a) to (d)). The biological processes category exhibited a noteworthy enrichment of genes primarily associated with regulating transcription, intracellular signal transduction, and protein ubiquitination (Figure 5(e)). Genes within the molecular function category exhibited enrichment in DNA

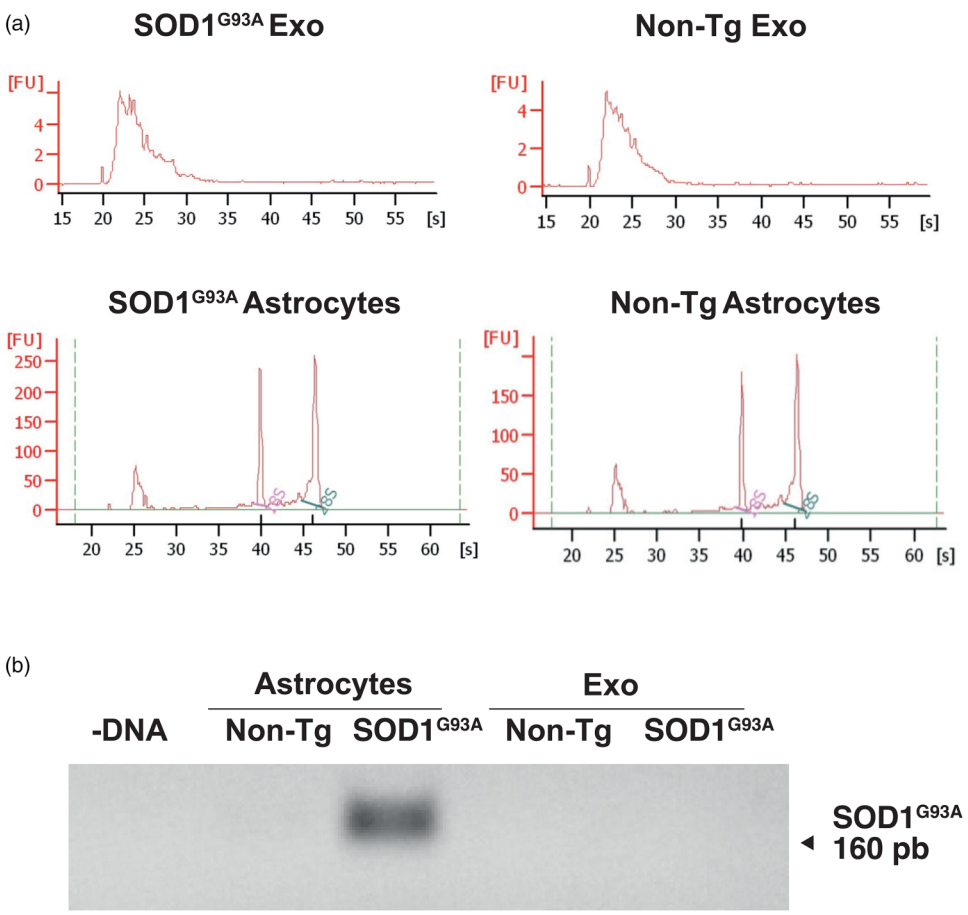

Figure 2. Human SOD1^{G93A} mRNA is undetectable in exosomes of SOD1^{G93A} astrocytes. (a) Electropherogram results of total RNA extracted with TRIzol. (b) SOD1^{G93A} mRNA expression in non-Tg and SOD1^{G93A} astrocytes and astrocyte-derived exosomes, as assessed by RT-PCR.

binding, protein binding, and chromatin binding, as indicated in Figure 5(d). In the cellular component enrichment analysis, most of the target genes were associated with the nuclear compartment except for a reduced but significant set that localized to the cytosol (Figure 5(c)). Additionally, 123 genes were detected in KEGG pathway enrichment analysis, most of them related to signaling pathways. Neurotrophin signaling (KEGG: 04722, with a p-value of 0.00005 and FDR of 0.003) was among the top five enriched pathways (Figure 5(b)). Furthermore, we found that key factors such as PI3 K, Ras, or NFκB of neurotrophin signaling were putatively regulated by miR-155-5p (Supplemental Figure 2), which could be the effect observed on MN survival and neurite length.

On the other hand, miR-582-3p predicted target gene analyses identified 730 putative targets with TargetScan and 3,310 with DIANA-microT-CDS software, of which 628 were predicted with both algorithms (Figure 6(a)). The enrichment analysis showed no enrichment in the biological process category, only one term in molecular function, protein binding (FDR = 0.00003), and several enriched terms in the cellular component category. KEGG pathway enrichment analysis only identified the neurotrophin pathway as a pathway enriched in miR-582-3p target genes (Figure 6(b) to (d)).

SOD1^{G93A} Astrocyte-Derived Exosome-Mediated MN Death Was Reduced by Depletion of miR-155-5p

Due to the overexpression of miR-155-5p in SOD1^{G93A} exosomes and its involvement in neurotrophin signaling pathways with more putative targets compared to miR-582-3p, we conducted further analysis to investigate the role of miR-155-5p in MN death induced by SOD1^{G93A} astrocyte exosomes. Primary MNs were incubated with astrocyte exosomes (non-Tg or SOD1^{G93A}) together with miR-155-5p mimics or miR-155-5p inhibitors, and cell survival and neurite branching were analyzed (Figure 7(a)). Interestingly, when MNs were treated with non-Tg astrocyte-derived exosomes in the presence of a miR155-5p mimetic, a reduction in MN survival was observed (Exo-non-Tg-miR, 64.16 ± 20.07%). Importantly, when MNs were treated with exosomes

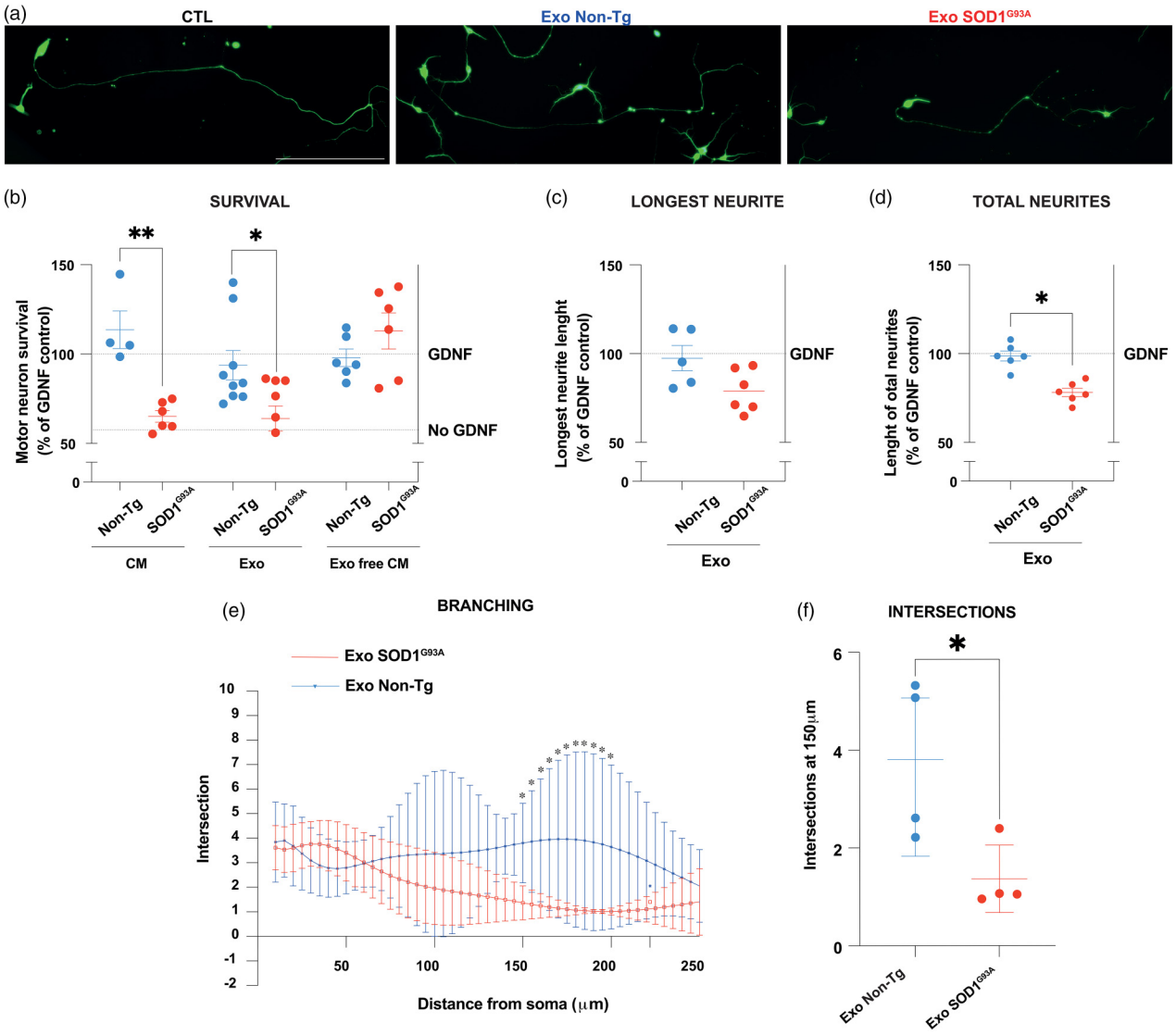

Figure 3. SOD1^{G93A} astrocyte-derived exosomes reduce MN survival, neurite length, and neurite branching. (a) Representative images of primary cultures of MNs treated with GDNF (1 ng/ml, CTL) or with GDNF and exosomes from non-Tg or SOD1^{G93A} astrocytes. MNs were immunostained with beta III tubulin, scale bar = 250 μm. (b) MN survival after treatment with GDNF and following the addition of the indicated CM (non-Tg and SOD1^{G93A}), exosomes (Exo; non-Tg and SOD1^{G93A}) or CM depleted of exosomes (Exo free CM; non-Tg and SOD1^{G93A}). Data are expressed as a percentage of survival after GDNF addition (100%, upper dotted line) compared to MN survival with no addition of trophic factor (lower dotted line). Unpaired *t*-tests were carried out, and the levels of significance were represented as $*p < .05$, $**p < .01$. (c) and (d) Longest neurite length and total neurite length plot. MNs were treated with GDNF (control) and with GDNF and exosomes from nontransgenic and SOD1^{G93A} astrocytes (Exo; non-Tg and SOD1^{G93A}). At least seven neurites per treatment were quantified with the Fiji program. Data are expressed as the mean ± SEM from five to six independent experiments (GDNF, Exo; non-Tg and SOD1^{G93A}). Unpaired *t*-tests were performed, and significance levels were denoted as unpaired *t*-tests, $*p < .05$. (e) Representative images of Sholl graphs of MNs treated with exosomes. Mean ± SEM from at least three independent experiments. A two-way ANOVA followed by Fisher's LSD test for multiple comparisons was performed. $p < .05$ was used to determine statistical significance. (f) Intersections at 150 μm from the soma. An unpaired *t*-test was used to analyze the significant branching of neurites at 150 μm. An unpaired *t*-test was executed, and the significance levels were indicated as follows: $*p < .05$. Experiments performed with non-Tg astrocyte fractions are depicted in blue, and those from SOD1^{G93A} ones are in red.

of SOD1^{G93A} astrocytes and transfected with oligonucleotides that inhibit miR-155-5p, MN death induced by SOD1^{G93A} astrocyte exosomes was not detected (Exo-SOD1^{G93A}-αmiR, 50.51 ± 19.42%; Exo-SOD1^{G93A} 104.45 ± 21.61%; Figure 7(a)). Conversely, when MNs were treated with exosomes of non-Tg astrocytes in the presence of miR155-5p inhibitors or SOD1^{G93A} astrocytes in the presence of miR-155-5p mimetics, no differences were found compared to those with the

Table 2. Analyzed miRNAs in Astrocytes or Astrocyte-Derived Exosomes.

MicroRNA	Astrocytes	Exosomes	References
miR-9	Yes	No	(Campos-Melo et al., 2018; Haramati et al., 2010; Hawley et al., 2019; Marcuzzo et al., 2015, 2014; Saucier et al., 2019; Zhang et al., 2013)
miR-23a	No	ND	(Russell et al., 2013)
miR-124	Yes	No	(Cunha et al., 2018; Marcuzzo et al., 2015; Morel et al., 2013)
miR-132	Yes	No	(Freischmidt et al., 2014)
miR-155-5p	Yes	Yes	(Cunha et al., 2018; Koval et al., 2013)
miR-582-3p	Yes	Yes	(Campos-Melo et al., 2013)

Yes = detected by RT-SL qPCR amplification, no = no detection in RT-SL qPCR, ND = not determined.

respective exosomes alone (Exo-non-Tg-αmiR 116.98 ± 2.86%; Exo-SOD1^{G93A}-miR 16.31 ± 5.50%). In addition, no significant effect on MN survival was detected when adding either the miRNA or the antisense miRNA alone (miR, 70.24 ± 32.06%; αmiR 155-5p, 92.74 ± 80.97% compared to MNs treated with non-Tg astrocyte exosomes). Interestingly, MN branching was increased when MNs were treated with SOD1^{G93A} astrocyte-derived exosomes in the presence of miR-155-5p inhibitors compared to the one developed when treated with the SOD1^{G93A} astrocyte-derived exosomes alone (Figure 7(b) and (c)).

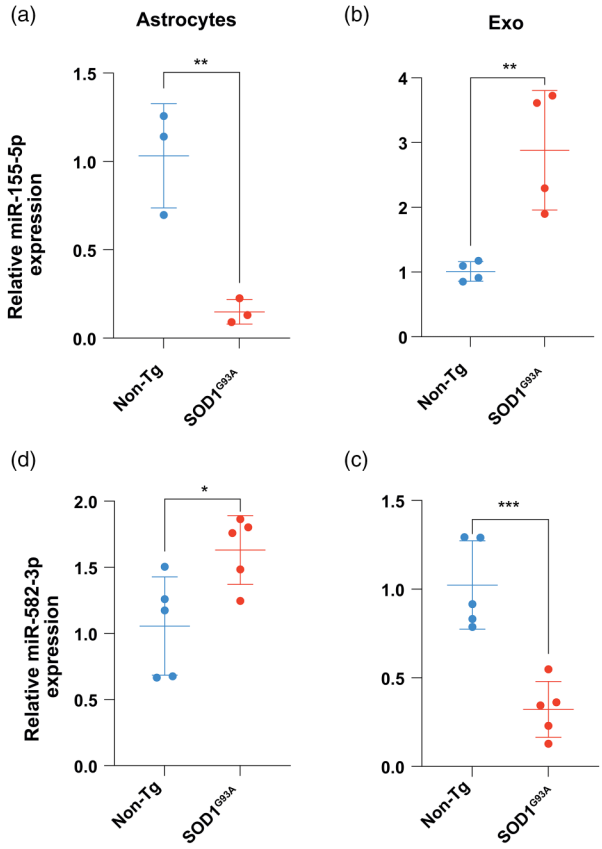

Figure 4. miR-155-5p and miR-582-3p show different expression levels in SOD1^{G93A} and non-Tg astrocyte exosomes. (a) and (c) Relative expression levels of miR-155-5p and miR-582-3p in astrocytes. (b) and (d) Relative expression levels of miR-155-5p and miR-582-3p in astrocyte exosomes. qRT-PCR quantification was performed with the ΔΔCt method using non-Tg samples as negative control and GAPDH mRNA as an endogenous reference control. Data are the mean ± SEM from at least three independent experiments. Unpaired *t*-tests were performed, and significance levels were denoted as *$p < .05$, **$p < .01$, ***$p < .005$.

Discussion

In the present work, we demonstrate that SOD1^{G93A} astrocyte-derived exosomes are sufficient to reduce neurite outgrowth and survival of MNs in the presence of GDNF to the level exhibited upon trophic factor deprivation. In addition, we provide evidence that miRNA 155-5p contributes to SOD1^{G93A} exosome-mediated MN death.

The fraction isolated from CM of primary SOD1^{G93A} and non-Tg astrocyte cultures contained round-shaped vesicles of 60–100 nm diameter and carried flotillin-1 and ESCRT-I complex component, TSG101, consistent with previously reported exosome features (De Gassart et al., 2003; Thery et al., 1999). Following prior findings, the exosomes derived from SOD1^{G93A} astrocytes contained human SOD1 protein (Basso et al., 2013; Silverman et al., 2019). Exosomes containing mutated or misfolded SOD1 are reported to be secreted by MNs, astrocytes, and microglia (Basso et al., 2013; Gomes et al., 2007; Massenzio et al., 2018; Vaz et al., 2019). Mutated or misfolded SOD1 decorates the surface of exosomes and can be transferred to healthy cells (Silverman et al., 2019). In addition, proteins associated with ALS such as VCP, TDP43, FUS, other RNA-binding proteins, and dipeptide repeats (DPRs) resulting from C9orf72 expansions have been described to be present in exosomes derived from cells overexpressing these proteins (Basso et al., 2013; Iguchi et al., 2016; Nonaka et al., 2013). While some researchers have suggested that this could be a mechanism of maintaining cell survival by conveying toxic materials including misfolded proteins out of the cell (Desdín-Micó & Mittelbrunn, 2017), others have suggested that exosomes may propagate toxicity in ALS (Basso et al., 2013; Ding et al., 2015; Grad & Cashman, 2014; Westergard et al., 2016). This work shows that the toxic effects of SOD1^{G93A} astrocyte-derived exosomes on MNs could be related to miRNA cargo.

Earlier studies have indicated that astrocytes derived from mutant SOD1 mice (Nagai et al., 2007) and rats (Vargas et al., 2006) can induce MN death *in vitro* by releasing soluble

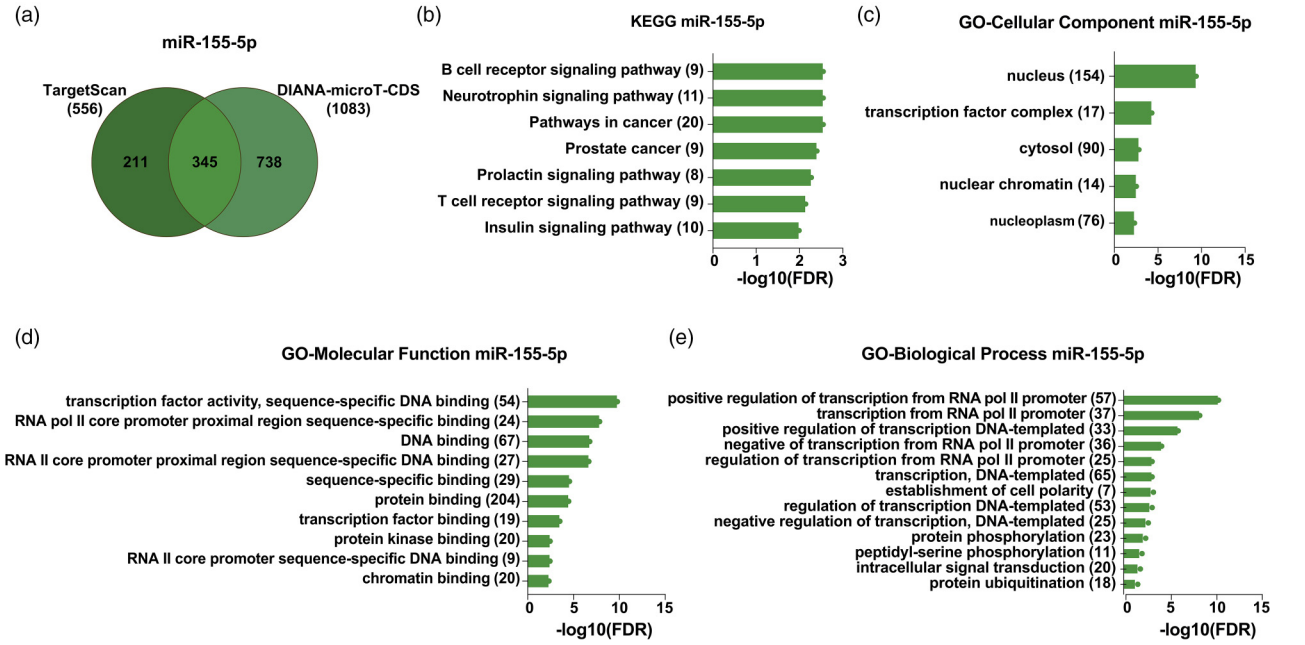

Figure 5. Enrichment analysis of miR-155-5p predicted targets. (a) Venn diagram of miR-155-5p predicted targets with TargetScan and DIANA-microT-CDS. (b) Enrichment analysis of KEGG pathways (123), (c) cellular component (322), (d) molecular function (309), and (e) biological process (309) in terms of miR-155-5p predicted targets. The *x*-axis represents the enrichment value as a −10 logarithm of the adjusted *p*-value (FDR). The number of genes identified in each pathway is reported inside parentheses. All represented KEGG and GO terms are significantly enriched, with an adjusted *p*-value < .05 and FDR < 0.05. KEGG = Kyoto Encyclopedia of Genes and Genomes.

specific factors present in CM. Numerous agents have been suggested to participate in this toxicity, including nitric oxide, ATP (Almad et al., 2016; Gandelman et al., 2010), lipids (Guttenplan et al., 2021), or proteins such as pro–nerve growth factor (proNGF) (Pehar et al., 2017) and amyloid precursor protein (Mishra et al., 2020). However, the exact mechanism of MN death and the nature of these toxic factors remain elusive and subject to ongoing debate (Van Harten et al., 2021). In this context, $SOD1^{G93A}$ and non-Tg astrocyte-derived exosomes are taken up by cultured MNs and induce MN death *in vitro* when applied to non-Tg spinal neuron-astrocyte cocultures (Basso et al., 2013). Moreover, SOD1 astrocyte-derived exosomes have been described to induce MN death *in vitro* when applied to non-Tg spinal neuron–astrocyte cocultures (Basso et al., 2013), and EVs from astrocytes derived from fibroblasts of C9orf72 ALS patients are also toxic to MNs (Varcianna et al., 2019). Here, we show that the $SOD1^{G93A}$ astrocyte-derived exosomes are sufficient to induce MN death and reduce neurite outgrowth in purified MN cultures, suggesting that these exosomes could contribute to astrocyte-mediated MN toxicity.

Basso et al. showed that the $SOD1^{G93A}$ protein carried by exosomes is transferred to spinal neurons while the $SOD1^{G93A}$ present in exosome-free astrocyte CM is undetectable inside spinal neurons (Basso et al., 2013). Besides protein content, exosomes are reported to carry important RNA species where they exhibit increased stability and protection from RNase (Ratajczak et al., 2006; Valadi et al., 2007) and may also affect neuronal survival. The analysis of exosomal RNA cargo revealed a broad range of RNA sizes in non-Tg and SOD^{1G93A} astrocyte-derived exosomes. As previously described for exosomal RNAs (Valadi et al., 2007), the sizes of 18S and 28S ribosomal RNAs in astrocyte exosomes were undetectable, but they were present in astrocyte cells. We focused on miRNAs because of previous reports suggesting their involvement in ALS (Campos-Melo et al., 2013; De Felice et al., 2012; Emde et al., 2015; Hoye et al., 2017; Koval et al., 2013; Zhou et al., 2013) and its essential role in gene expression regulation. Moreover, some miRNAs were reported to be altered in ALS such as miR-9, miR-23a, miR-124, miR-132, miR-155-5p, and miR-582-3p (Campos-Melo et al., 2013, 2018; Cunha et al., 2018; Freischmidt et al., 2014; Haramati et al., 2010; Hawley et al., 2019; Koval et al., 2013; Marcuzzo et al., 2015, 2014; Morel et al., 2013; Russell et al., 2013; Saucier et al., 2019; Zhang et al., 2013).

These miRNA species, except for miR-23a, were identified in cultured astrocytes. In addition, previous studies have reported that these miRNAs, except for miR-132, are deregulated in the spinal cords of ALS patients with mutations in SOD1, TARDBP, FUS/TLS, expanded repeats on C9ORF72 (Butovsky et al., 2012; Campos-Melo et al., 2018; Freischmidt et al., 2014; Hawley et al., 2019; Koval et al., 2013; Zhang et al., 2013), or $SOD1^{G93A}$ murine models (Cunha et al., 2018; Marcuzzo et al., 2015, 2014;

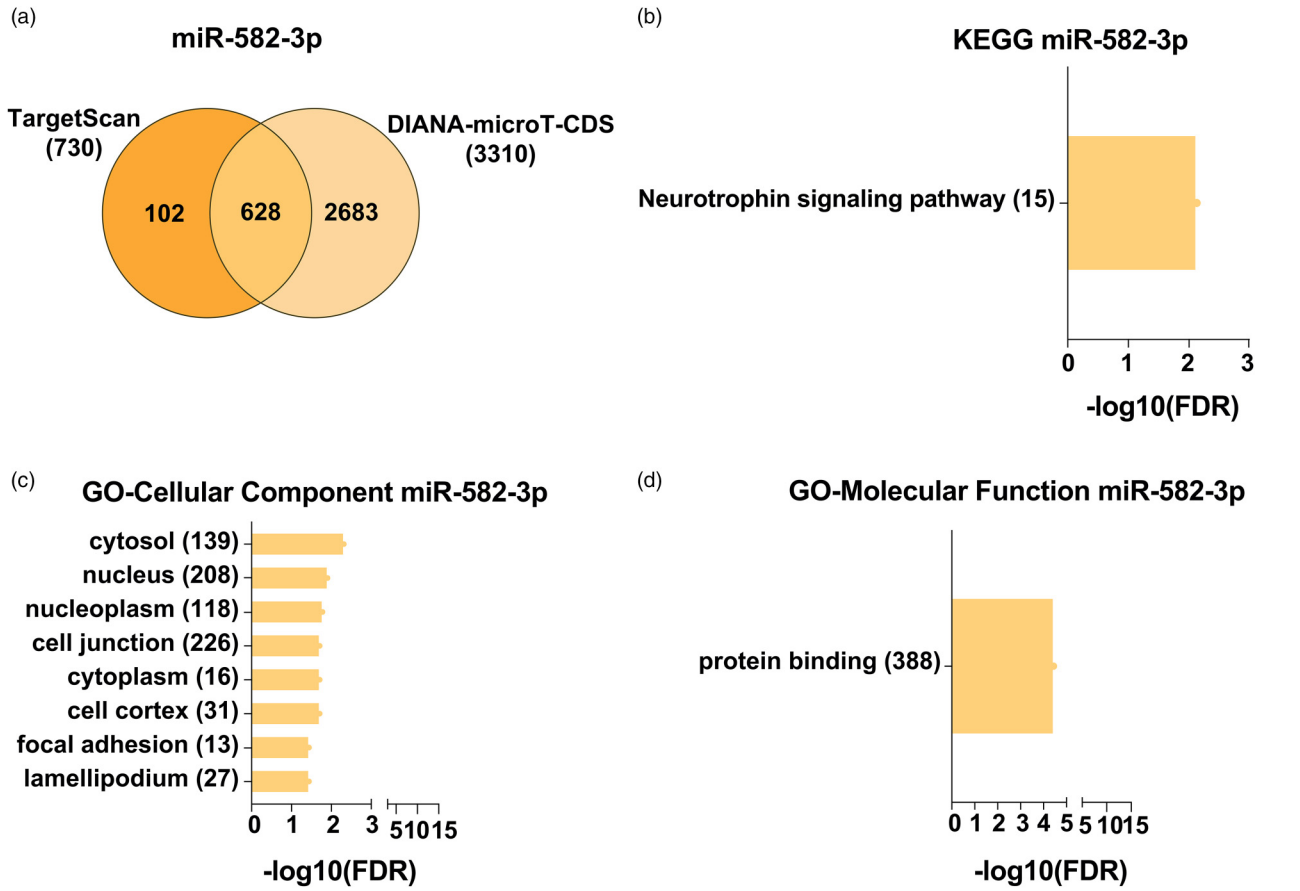

Figure 6. Enrichment analysis of miR-582-3p predicted targets. (a) Venn diagram of miR-582-3p predicted targets with TargetScan and DIANA-microT-CDS. (b) Enrichment analysis of KEGG pathways (199), (c) cellular component (538), and (d) molecular function (526), in terms of miR-582-3p predicted targets. The *x*-axis represents the enrichment value as the −10 logarithm of the adjusted *p*-value (FDR). The number of genes identified in each pathway is reported inside parentheses. All represented KEGG and GO terms are significantly enriched, with an adjusted *p*-value < .05, and FDR< 0.05. KEGG = Kyoto Encyclopedia of Genes and Genomes.

Morel et al., 2013). miR-132, on the other hand, is downregulated in cerebrospinal fluid and serum of sporadic ALS cases with mutations in TARDBP, FUS, and C9ORF72, but not SOD1 mutant patients (Freischmidt et al., 2014). Interestingly, only miR-155-5p and miR-582-3p were observed in astrocyte-derived exosomes, and quantitative PCR of miR-155-5p and miR-582 showed different miRNA expression levels in SOD1^{G93A} astrocytes relative to non-Tg cells. Moreover, miRNA levels of miR-155-5p and miR-582-3p in astrocyte-derived exosomes are different than in astrocytes. This agrees with data reported in the literature showing that exosome miRNA expression profiles are functionally different from those of the parent cells (Zhang et al., 2015). Particularly, significant differences were observed in miRNA profiles between mouse astrocyte-derived exosomes compared to whole-cell astrocytes (Jovicic & Gitler, 2017).

Concerning both miRNAs present in astrocyte exosomes, this is the first report of miR-582-3p levels in astrocytes or astrocyte EVs. Notably, it is downregulated in the spinal cord of ALS patients with mutations in SOD1, TARDBP, FUS/TLS, or expanded repeats on C9ORF72 (Campos-Melo et al., 2013). The downregulation of miR-582-3p found in the exosomes of SOD1^{G93A} astrocytes could be relevant in pathological spreading in ALS due to its regulatory role in physiologically relevant mRNA expression (Campos-Melo et al., 2013; Qin et al., 2018). On the other hand, miR-155 has been observed to be overexpressed in the spinal cord of familial and sporadic ALS patients as well as in the spinal cord of SOD1^{G93A} mice at presymptomatic and symptomatic stages and has been suggested as an early marker of disease (Cunha et al., 2018). However, no differences were reported in miR-155-5p expression levels at the cerebral cortex between SOD1^{G93A} and non-Tg mice (Gomes et al., 2019). In addition, miR-155-5p was detected in small EVs derived from astrocytes (Gomes et al., 2020). In this study, we observed a downregulation of miR-155-5p in cultured SOD1^{G93A} astrocytes, while there was an upregulation of miR-155-5p in the SOD1^{G93A} astrocyte exosomes. miR-155-5p has numerous suggested and validated targets

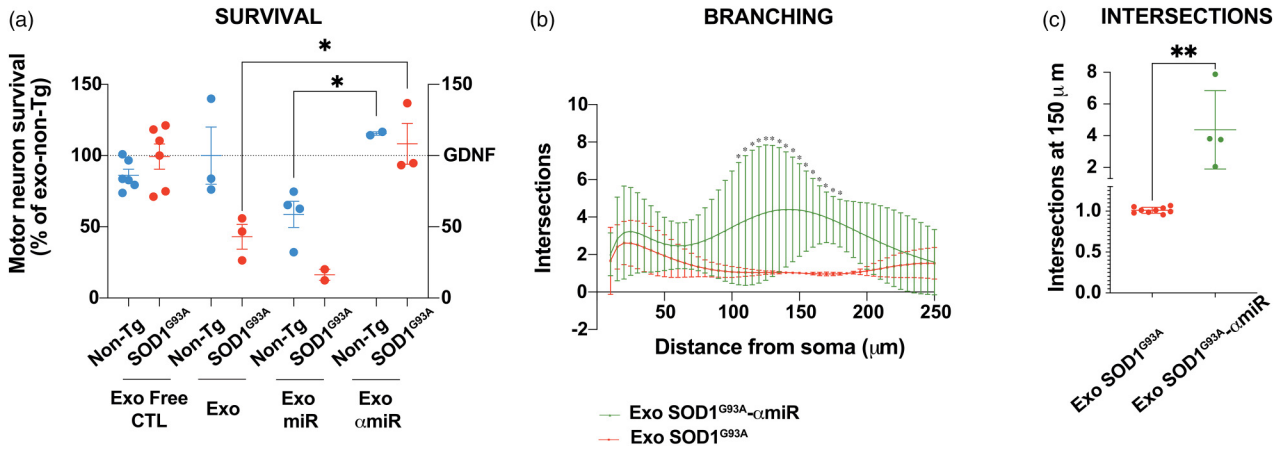

Figure 7. Inhibition of miR-155-5p rescue MN death induced by SOD1^{G93A} astrocyte exosomes. MN survival 24 h after incubation with SOD1^{G93A} (red) or non-Tg (blue) exosomes plus the miR155-5p mimic or inhibitor as indicated. Data show the percentage of MNs compared to control (MNs treated with non-Tg astrocyte exosomes). 24 h primary MN cultures were treated with non-Tg CM depleted of exosomes from non-Tg and SOD1^{G93A} astrocytes (Exo free CM; non-Tg, and SOD1^{G93A}, respectively), or with exosomes of non-Tg and SOD1^{G93A} astrocytes (Exo; non-Tg and SOD1^{G93A}, respectively), cotransfected with miR-155-5p mimetics (Exo miR; non-Tg or SOD1^{G93A}) or miR-155-5p inhibitors (α-miR; non-Tg and SOD1^{G93A}). Mean ± SEM from at least three independent experiments. One-way ANOVA results: *$p < .05$, from non-Tg treated control. (b) Representative images of Sholl graphs of MNs treated with exosomes from SOD1^{G93A} astrocytes (Exo-SOD1^{G93A}) in the absence or presence of miR-155-5p inhibitors (Exo-SOD1^{G93A}-αmiR). Mean ± SEM from at least three independent experiments. A two-way ANOVA followed by Fisher's LSD test for multiple comparisons was performed. $p < .05$ was employed to determine statistical significance. (c) Intersections at 150 μm from the soma. An unpaired *t*-test was used to analyze the significant branching of neurites at 150 μm. Experiments performed with Exo-SOD1^{G93A} astrocytes are depicted in red, and those from Exo-SOD1^{G93A}-αmiR ones are in green. An unpaired *t*-test was conducted, and the results were denoted as *$p < .05$, **$p < .01$, and ***$p < .005$.

(Bayraktar et al., 2015). Its synthesis is stimulated by proinflammatory cytokines such as TNF-α, which activates NF-κB transcription factor that promotes miR-155-5p biogenesis (Lee et al., 2014; Kim et al., 2017). In astrocytes, it is upregulated after IL-1 or TNFα cytokine stimulation, leading to a neurotoxic astrocyte phenotype (Tarassishin et al., 2011).

In silico target analysis identified 341 putative targets for miR-155-5p and 628 for miR-582-3p. In both cases, pathways of targeted mRNAs identified by KEGG analysis revealed an increment in neurotrophin signaling pathway-related genes. Given that miR-155-5p showed a higher number of putative targets than miR-582-3p, our study focused on exploring the implications of miR-155-5p. As for miR-582-3p, further investigations will be carried out to elucidate its involvement in astrocyte-mediated MN death.

Our study reveals that inhibiting miR-155 effectively decreased the death of MNs induced by SOD1^{G93A} astrocyte-derived exosomes, resulting in similar survival rates to MNs treated with exosomes from nontransgenic (non-Tg) astrocytes. Additionally, we observed a significant enhancement in the growth and branching of MN neurites. This result is consistent with the KEGG analysis, which identified an increase in neurotrophin signaling pathways. Neurotrophins are trophic factors that promote neuronal survival and development and significantly regulate axonal and dendritic growth (Park & Poo, 2013). Furthermore, these findings align with previous research showing that primary cultures of dorsal root neurons from miR-155 knockout (KO) mice displayed an approximate 40% increase in neurite length, indicating enhanced arborization (Gaudet et al., 2016). Following peripheral injury, miR-155-5p KO mice show higher regenerative levels than those observed in control mice. These results are associated with an improvement in motor skills after nerve contusion (Gaudet et al., 2016). In addition, inhibition of miR-155-5p by intraventricular administration of anti-miR-155 in SOD1^{G93A} mice significantly extended survival (Koval et al., 2013). Our results provide further evidence supporting the toxic activity of miR-155-5p toward MNs. Nonetheless, additional research is required to determine whether neurotrophin signaling pathway-related genes undergo modifications in recipient MNs when EVs derived from SOD1^{G93A} astrocytes are applied.

In summary, our results show that miR-155-5p expression is increased in SOD1^{G93A} astrocyte-derived exosomes and that these exosomes critically influence MN survival in culture, describing a new mechanism by which astrocytes may contribute to MN death in ALS. Moreover, these data suggest a potential new therapeutic target to modify disease outcomes in ALS consistent with previous reports (Koval et al., 2013).

Conclusion

The exosomes derived from astrocytes overexpressing the ALS-linked mutant Cu/Zn superoxide dismutase

(SOD1^{G93A}) are enriched with miRNA-155-5p. In addition, miR-155-5p reduces the ability of exosomes derived from non-Tg astrocytes to support MN survival.

Abbreviations

ALS	amyotrophic lateral sclerosis
C9ORF72	chromosome 9 open reading frame 72
CM	conditioned medium
ESCRT-I	endosomal sorting complex responsible for transport 1
EVs	extracellular vesicles
FUS	fused in sarcoma
GDNF	glial cell-derived neurotrophic factor
GFAP	glial fibrillary acidic protein
KEGG	Kyoto Encyclopedia of Genes and Genomes
miR	microRNA
MN	motor neuron
mRNA	messenger RNA
MV	microvesicles
MVB	multivesicular bodies
p100	pellet fraction from 100000×*g* ultracentrifugation
rRNA	ribonucleic acid RNA
SOD1^{G93A}	human gene SOD1 with a glycine to alanine substitution in position 93
TDP-43	TAR DNA binding protein-43
TSG101	tumor susceptibility gene 101.

Acknowledgments

The data presented herein were obtained using instrumentation in the Microscopy Unit of Facultad de Medicina, Universidad de la República, Montevideo, with the support of Core staff. The facility is funded through user fees and financial support. We would like to thank Dr. Luciana Negro from the School of Biomedical Engineering, Sciences and Health Systems, Drexel University, Philadelphia; Dr. Zachary Fitzpatrick from Spark Therapeutics, Philadelphia, for kindly reading the manuscript and comments; Dr. José Tort from Facultad de Medicina, Universidad de la República, Montevideo, for bioinformatic assistance; Dr. Juan Pablo Tosar and MSc Pablo Fagúndez from Facultad de Ciencias, Universidad de la República, Montevideo, for the analysis and quantification of exosomes; and Dr. Carlos Robello from Institut Pasteur, Montevideo, Uruguay, for support in the analysis of exosomal RNA.

Author Contribution

Project conceptualization and design were developed by S.M., E.M., and P.C. Experiments and analyses were performed by S.M., E.M., J.A., and S.F. The manuscript was written and edited by S.M. and P.C.

Declaration of Conflicting Interests

The authors declared no potential conflicts of interest with respect to the research, authorship, and/or publication of this article.

Funding

The authors disclosed receipt of the following financial support for the research, authorship, and/or publication of this article: This work was supported by a research fellowship award from Agencia Nacional de Investigación e Innovación (ANII) (PD NAC 2014,1,102084) to S.M. and by ANII grant [FCE_1_2014_1_104239] to P.C.

ORCID iD

Soledad Marton https://orcid.org/0000-0001-9007-3104

Supplemental Material

Supplemental material for this article is available online.

References

Agarwal, V., Bell, G. W., Nam, J. W., & Bartel, D. P. (2015). Predicting effective microRNA target sites in mammalian mRNAs. *elife*, *4,* e05005. https://doi.org/10.7554/eLife.05005

Almad, A. A., Doreswamy, A., Gross, S. K., Richard, J. P., Huo, Y., Haughey, N., & Maragakis, N. J. (2016). Connexin 43 in astrocytes contributes to motor neuron toxicity in amyotrophic lateral sclerosis. *Glia*, *64*(7), 1154–1169. https://doi.org/10.1002/glia.22989

Ambros, V. (2004). The functions of animal microRNAs. *Nature*, *431*(7006), 350–355. https://doi.org/10.1038/nature02871

Arab, T., Mallick, E. R., Huang, Y., Dong, L., Liao, Z., Zhao, Z., Gololobova, O., Smith, B., Haughey, N. J., Pienta, K. J., Slusher, B. S., Tarwater, P. M., Tosar, J. P., Zivkovic, A. M., Vreeland, W. N., Paulaitis, M. E., & Witwer, K. W. (2021). Characterization of extracellular vesicles and synthetic nanoparticles with four orthogonal single-particle analysis platforms. *Journal of Extracellular Vesicles*, *10*(6), e12079. https://doi.org/10.1002/jev2.12079

Arnold, E. S., Ling, S. C., Huelga, S. C., Lagier-Tourenne, C., Polymenidou, M., Ditsworth, D., Kordasiewicz, H. B., McAlonis-Downes, M., Platoshyn, O., Parone, P. A., Da Cruz, S., Clutario, K. M., Swing, D., Tessarollo, L., Marsala, M., Shaw, C. E., Yeo, G. W., & Cleveland, D. W. (2013). ALS-linked TDP-43 mutations produce aberrant RNA splicing and adult-onset motor neuron disease without aggregation or loss of nuclear TDP-43. *Proceedings of the National Academy of Sciences of the United States of America*, *110*(8), E736–E745. https://doi.org/10.1073/pnas.1222809110

Barbeito, L. H., Pehar, M., Cassina, P., Vargas, M. R., Peluffo, H., Viera, L., Estévez, A. G., & Beckman, J. S. (2004). A role for astrocytes in motor neuron loss in amyotrophic lateral sclerosis. *Brain Research Reviews*, *47*(1-3), 263–274. https://doi.org/10.1016/j.brainresrev.2004.05.003

Bartel, D. P. (2004). MicroRNAs: Genomics, biogenesis, mechanism, and function. *Cell*, *116*(2), 281–297. https://doi.org/10.1016/S0092-8674(04)00045-5

Basso, M., Pozzi, S., Tortarolo, M., Fiordaliso, F., Bisighini, C., Pasetto, L., Spaltro, G., Lidonnici, D., Gensano, F., Battaglia, E., Bendotti, C., & Bonetto, V. (2013). Mutant copper-zinc superoxide dismutase (SOD1) induces protein secretion pathway alterations and exosome release in astrocytes. *Journal of Biological Chemistry*, *288*(22), 15699–15711. https://doi.org/10.1074/jbc.M112.425066

Bayraktar, O. A., Fuentealba, L. C., Alvarez-Buylla, A., & Rowitch, D. H. (2015). Astrocyte development and heterogeneity. *Cold Spring Harbor Perspectives in Biology*, *7*(1), a020362. https://doi.org/10.1101/cshperspect.a020362

Bilsland, L. G., Sahai, E., Kelly, G., Golding, M., Greensmith, L., & Schiavo, G. (2010). Deficits in axonal transport precede ALS symptoms in vivo. *Proceedings of the National Academy of Sciences of the United States of America*, *107*(47), 20523–20528. https://doi.org/10.1073/pnas.1006869107

Boillée, S., Yamanaka, K., Lobsiger, C. S., Copeland, N. G., Jenkins, N. A., Kassiotis, G., Kollias, G., & Cleveland, D. W. (2006). Onset and progression in inherited ALS determined by motor neurons and microglia. *Science*, *312*(5778), 1389–1392. https://doi.org/10.1126/science.1123511

Brown, R. H., & Al-Chalabi, A. (2017). Amyotrophic lateral sclerosis longo DL, ed. *New England Journal of Medicine*, *377*(2), 162–172. https://doi.org/10.1056/NEJMra1603471

Butovsky, O., Siddiqui, S., Gabriely, G., Lanser, A. J., Dake, B., Murugaiyan, G., Doykan, C. E., Wu, P. M., Gali, R. R., Iyer, L. K., Lawson, R., Berry, J., Krichevsky, A. M., Cudkowicz, M. E., & Weiner, H. L. (2012). Modulating inflammatory monocytes with a unique microRNA gene signature ameliorates murine ALS. *Journal of Clinical Investigation*, *122*(9), 3063–3087. https://doi.org/10.1172/JCI62636

Campos-Melo, D., Droppelmann, C. A., He, Z., Volkening, K., & Strong, M. J. (2013). Altered microRNA expression profile in amyotrophic lateral sclerosis: A role in the regulation of NFL mRNA levels. *Molecular Brain*, *6*(1), 362–375. https://doi.org/10.1186/1756-6606-6-26

Campos-Melo, D., Hawley, Z. C. E., & Strong, M. J. (2018). Dysregulation of human NEFM and NEFH mRNA stability by ALS-linked miRNAs. *Molecular Brain*, *11*(1), 9655–9664. https://doi.org/10.1186/s13041-018-0386-3

Cassina, P., Peluffo, H., Pehar, M., Martínez-Palma, L., Ressia, A., Beckman, J. S., Estévez, A. G., & Barbeito, L. (2002). Peroxynitrite triggers a phenotypic transformation in spinal cord astrocytes that induces motor neuron apoptosis. *Journal of Neuroscience Research*, *67*(1), 21–29. https://doi.org/10.1002/jnr.10107

Ceruti, S., Colombo, L., Magni, G., Vigano, F., Boccazzi, M., Deli, M. A., Sperlagh, B., Abbracchio, M. P., & Kittel, A. (2011). Oxygen-glucose deprivation increases the enzymatic activity and the microvesicle-mediated release of ectonucleotidases in the cells composing the blood-brain barrier. *Neurochemistry International*, *59*(2), 259–271. https://doi.org/10.1016/j.neuint.2011.05.013

Chandler, C. E., Parsons, L. M., Hosang, M., & Shooter, E. M. (1984). A monoclonal antibody modulates the interaction of nerve growth factor with PC12 cells. *Journal of Biological Chemistry*, *259*(11), 6882–6889. https://doi.org/10.1016/S0021-9258(17)39810-1

Chen, X., He, X., Yang, Y. Y., & Wang, Y. (2022). Amyotrophic lateral sclerosis-associated mutants of SOD1 modulate miRNA biogenesis through aberrant interactions with exportin 5. *ACS Chemical Biology*, *17*(12), 3450–3457. https://doi.org/10.1021/acschembio.2c00591

Clement, A. M., Nguyen, M. D., Roberts, E. A., Garcia, M. L., Boillée, S., Rule, M., McMahon, A. P., Doucette, W., Siwek, D., Ferrante, R. J., Brown, R. H., Julien, J.-P., Goldstein, L. S. B., & Cleveland, D. W. (2003). Wild-type nonneuronal cells extend survival of SOD1 mutant motor neurons in ALS mice. *Science*, *302*(5642), 113–117. https://doi.org/10.1126/science.1086071

Cunha, C., Santos, C., Gomes, C., Fernandes, A., Correia, A. M., Sebastiao, A. M., Vaz, A. R., & Brites, D. (2018). Downregulated glia interplay and increased miRNA-155 as promising markers to track ALS at an early stage. *Molecular Neurobiology*, *55*(5), 4207–4224. https://doi.org/10.1007/s12035-017-0631-2

Da Cruz, S., & Cleveland, D. W. (2011). Understanding the role of TDP-43 and FUS/TLS in ALS and beyond. *Current Opinion in Neurobiology*, *21*(6), 904–919. https://doi.org/10.1016/j.conb.2011.05.029

De Felice, B., Guida, M., Guida, M., Coppola, C., De Mieri, G., & Cotrufo, R. (2012). A miRNA signature in leukocytes from sporadic amyotrophic lateral sclerosis. *Gene*, *508*(1), 35–40. https://doi.org/10.1016/j.gene.2012.07.058

De Gassart, A., Géminard, C., Février, B., Raposo, G., & Vidal, M. (2003). Lipid raft-associated protein sorting in exosomes. *Blood*, *102*(13), 4336–4344. https://doi.org/10.1182/blood-2003-03-0871

Desdín-Micó, G., & Mittelbrunn, M. (2017). Role of exosomes in the protection of cellular homeostasis. *Cell Adhesion & Migration*, *11*(2), 127–134. https://doi.org/10.1080/19336918.2016.1251000

De Vos, K. J., & Hafezparast, M. (2017). Neurobiology of axonal transport defects in motor neuron diseases: Opportunities for translational research? *Neurobiology of Disease*, *105*, 283–299. https://doi.org/10.1016/j.nbd.2017.02.004

Díaz-Amarilla, P., Olivera-Bravo, S., Trias, E., Cragnolini, A., Martínez-Palma, L., Cassina, P., Beckman, J., & Barbeito, L. (2011). Phenotypically aberrant astrocytes that promote motoneuron damage in a model of inherited amyotrophic lateral sclerosis. *Proceedings of the National Academy of Sciences*, *108*(44), 18126–18131. https://doi.org/10.1073/pnas.1110689108

Di Giorgio, F. P., Carrasco, M. A., Siao, M. C., Maniatis, T., & Eggan, K. (2007). Non-cell autonomous effect of glia on motor neurons in an embryonic stem cell-based ALS model. *Nature Neuroscience*, *10*(5), 608–614. https://doi.org/10.1038/nn1885

Ding, X., Ma, M., Teng, J., Teng, R. K. F., Zhou, S., Yin, J., Fonkem, E., Huang, J. H., Wu, E., & Wang, X. (2015). Exposure to ALS-FTD-CSF generates TDP-43 aggregates in glioblastoma cells through exosomes and TNTs-like structure. *Oncotarget*, *6*(27), 24178–24191. https://doi.org/10.18632/oncotarget.4680

Emde, A., et al. (2015). Dysregulated miRNA biogenesis downstream of cellular stress and ALS-causing mutations: A new mechanism for ALS. *EMBO Journal*, *34*(21), 2633–2651. https://doi.org/10.15252/embj.201490493

Falchi, A. M., Sogos, V., Saba, F., Piras, M., Congiu, T., & Piludu, M. (2013). Astrocytes shed large membrane vesicles that contain mitochondria, lipid droplets and ATP. *Histochemistry and Cell Biology*, *139*(2), 221–231. https://doi.org/10.1007/s00418-012-1045-x

Freischmidt, A., Müller, K., Ludolph, A. C., & Weishaupt, J. H. (2014). Systemic dysregulation of TDP-43 binding microRNAs in amyotrophic lateral sclerosis. *Acta Neuropathologica Communications*, *2*(1), 42. https://doi.org/10.1186/2051-5960-2-42

Fritz, E., Izaurieta, P., Weiss, A., Mir, F. R., Rojas, P., Gonzalez, D., Rojas, F., Brown, R. H., Madrid, R., & van Zundert, B. (2013). Mutant SOD1-expressing astrocytes release toxic factors that trigger motoneuron death by inducing hyperexcitability.

Journal of neurophysiology, *109*(11), 2803–2814. https://doi.org/10.1152/JN.00500.2012

Gandelman, M., Peluffo, H., Beckman, J. S., Cassina, P., & Barbeito, L. (2010). Extracellular ATP and the P2X7 receptor in astrocyte-mediated motor neuron death: Implications for amyotrophic lateral sclerosis. *Journal of Neuroinflammation*, *7*(1), 33. https://doi.org/10.1186/1742-2094-7-33

Gaudet, A. D., Mandrekar-Colucci, S., Hall, J. C. E., Sweet, D. R., Schmitt, P. J., Xu, X., Guan, Z., Mo, X., Guerau-De-Arellano, M., & Popovich, P. G. (2016). miR-155 deletion in mice overcomes neuron-intrinsic and neuron-extrinsic barriers to spinal cord repair. *Journal of Neuroscience*, *36*(32), 8516–8532. https://doi.org/10.1523/JNEUROSCI.0735-16.2016

Gharbi, T., Zhang, Z., & Yang, G.-Y. (2020). The function of astrocyte mediated extracellular vesicles in central nervous system diseases. *Frontiers in Cell and Developmental Biology*, *8*, 1–15. https://doi.org/10.3389/fcell.2020.568889

Gomes, C., Cunha, C., Nascimento, F., Ribeiro, J. A., Vaz, A. R., & Brites, D. (2019). Cortical neurotoxic astrocytes with early ALS pathology and miR-146a deficit replicate gliosis markers of symptomatic SOD1G93A mouse model. *Molecular Neurobiology*, *56*(3), 2137–2158. https://doi.org/10.1007/s12035-018-1220-8

Gomes, C., Keller, S., Altevogt, P., & Costa, J. (2007). Evidence for secretion of Cu,Zn superoxide dismutase via exosomes from a cell model of amyotrophic lateral sclerosis. *Neuroscience Letters*, *428*(1), 43–46. https://doi.org/10.1016/j.neulet.2007.09.024

Gomes, C., Sequeira, C., Barbosa, M., Cunha, C., Vaz, A. R., & Brites, D. (2020). Astrocyte regional diversity in ALS includes distinct aberrant phenotypes with common and causal pathological processes. *Experimental Cell Research*, *395*(2), 112209–112226. https://doi.org/10.1016/j.yexcr.2020.112209

Gorji-Bahri, G., Moradtabrizi, N., Vakhshiteh, F., & Hashemi, A. (2021). Validation of common reference genes stability in exosomal mRNA-isolated from liver and breast cancer cell lines. *Cell Biology International*, *45*(5), 1098–1110. https://doi.org/10.1002/cbin.11556

Grad, L. I., & Cashman, N. R. (2014). Prion-like activity of Cu/Zn superoxide dismutase implications for amyotrophic lateral sclerosis. *Prion*, *8*(1), 33–41. https://doi.org/10.4161/pri.27602

Gurney, M. E., Pu, H., Chiu, A. Y., Dal Canto, M. C., Polchow, C. Y., Alexander, D. D., Caliendo, J., Hentati, A., Kwon, Y. W., Deng, H.-X., Chen, W., Zhai, P., Sufit, R. L., & Siddique, T. (1994). Motor neuron degeneration in mice that express a human Cu,Zn superoxide dismutase mutation. *Science*, *264*(5166), 1772–1775. https://doi.org/10.1126/science.8209258

Guttenplan, K. A., Weigel, M. K., Prakash, P., Wijewardhane, P. R., Hasel, P., Rufen-Blanchette, U., Münch, A. E., Blum, J. A., Fine, J., Neal, M. C., Bruce, K. D., Gitler, A. D., Chopra, G., Liddelow, S. A., & Barres, B. A. (2021). Neurotoxic reactive astrocytes induce cell death via saturated lipids. *Nature*, *599*(7883), 102–107. https://doi.org/10.1038/s41586-021-03960-y

Hajrasouliha, A. R., Jiang, G., Lu, Q., Lu, H., Kaplan, H. J., Zhang, H.-G., & Shao, H. (2013). Exosomes from retinal astrocytes contain antiangiogenic components that inhibit laser-induced choroidal neovascularization. *Journal of Biological Chemistry*, *288*(39), 28058–28067. https://doi.org/10.1074/jbc.M113.470765

Haramati, S., Chapnik, E., Sztainberg, Y., Eilam, R., Zwang, R., Gershoni, N., McGlinn, E., Heiser, P. W., Wills, A. M., Wirguin, I., Rubin, L. L., Misawa, H., Tabin, C. J., Brown Jr., R., Chen, A., Hornstein, E., Brown Jr., R., Chen, A., & Hornstein, E. (2010). miRNA malfunction causes spinal motor neuron disease. *Proceedings of the National Academy of Sciences of the United States of America*, *107*(29), 13111–13116. https://doi.org/10.1073/pnas.1006151107

Hawley, Z. C. E., Campos-Melo, D., & Strong, M. J. (2019). miR-105 and miR-9 regulate the mRNA stability of neuronal intermediate filaments. Implications for the pathogenesis of amyotrophic lateral sclerosis (ALS). *Brain Research*, *1706*, 93–100. https://doi.org/10.1016/j.brainres.2018.10.032

Henderson, C. E., Camu, W., Mettling, C., Gouin, A., Poulsen, K., Karihaloo, M., Ruilamas, J., Evans, T., McMahon, S. B., Armanini, M. P., Berkemeier, L., Phillips, H. S., & Rosenthal, A. (1993). Neurotrophins promote motor neuron survival and are present in embryonic limb bud. *Nature*, *363*(6426), 266–270. https://doi.org/10.1038/363266a0

Howland, D. S., Liu, J., She, Y., Goad, B., Maragakis, N. J., Kim, B., Erickson, J., Kulik, J., DeVito, L., Psaltis, G., DeGennaro, L. J., Cleveland, D. W., & Rothstein, J. D. (2002). Focal loss of the glutamate transporter EAAT2 in a transgenic rat model of SOD1 mutant-mediated amyotrophic lateral sclerosis (ALS). *Proceedings of the National Academy of Sciences*, *99*(3), 1604–1609. https://doi.org/10.1073/pnas.032539299

Hoye, M. L., Koval, E. D., Wegener, A. J., Hyman, T. S., Yang, C., O'Brien, D. R., Miller, R. L., Cole, T., Schoch, K. M., Shen, T., Kunikata, T., Richard, J. P., Gutmann, D. H., Maragakis, N. J., Kordasiewicz, H. B., Dougherty, J. D., & Miller, T. M. (2017). MicroRNA profiling reveals marker of motor neuron disease in ALS models. *Journal of Neuroscience*, *37*(22), 5574–5586. https://doi.org/10.1523/JNEUROSCI.3582-16.2017

Huang, D. W., Sherman, B. T., & Lempicki, R. A. (2009). Systematic and integrative analysis of large gene lists using DAVID bioinformatics resources. *Nature Protocols*, *4*(1), 44–57. https://doi.org/10.1038/nprot.2008.211

Iguchi, Y., Eid, L., Parent, M., Soucy, G., Bareil, C., Riku, Y., Kawai, K., Takagi, S., Yoshida, M., Katsuno, M., Sobue, G., & Julien, J.-P. (2016). Exosome secretion is a key pathway for clearance of pathological TDP-43. *Brain*, *139*(12), 3187–3201. https://doi.org/10.1093/brain/aww237

Ilieva, H., Polymenidou, M., & Cleveland, D. W. (2009). Non-cell autonomous toxicity in neurodegenerative disorders: ALS and beyond. *Journal of Cell Biology*, *187*(6), 761–772. https://doi.org/10.1083/jcb.200908164

Jovicic, A., & Gitler, A. D. (2017). Distinct repertoires of microRNAs present in mouse astrocytes compared to astrocyte-secreted exosomes. *PLoS One*, *12*(2), e0171418. https://doi.org/10.1371/journal.pone.0171418

Kiernan, M. C., Vucic, S., Cheah, B. C., Turner, M. R., Eisen, A., Hardiman, O., Burrell, J. R., & Zoing, M. C. (2011). Amyotrophic lateral sclerosis. *The Lancet*, *377*(9769), 942–955. https://doi.org/10.1016/S0140-6736(10)61156-7

Kim, J., Lee, K. S., Kim, J. H., Lee, D. K., Park, M., Choi, S., Park, W., Kim, S., Choi, Y. K., Hwang, J. Y., Choe, J., Won, M. H., Jeoung, D., Lee, H., Ryoo, S., Ha, K. S., Kwon, Y. G., & Kim, Y. M. (2017). Aspirin prevents TNF-α-induced endothelial cell dysfunction by regulating the NF-κB-dependent miR-155/eNOS pathway: Role of a miR-155/eNOS axis in preeclampsia. *Free Radical Biology & Medicine*, *104*, 185–198. https://doi.org/10.1016/j.freeradbiomed.2017.01.010

Koval, E. D., Shaner, C., Zhang, P., du Maine, X., Fischer, K., Tay, J., Chau, B. N., Wu, G. F., & Miller, T. M. (2013). Method for widespread microRNA-155 inhibition prolongs survival in ALS-model mice. *Human Molecular Genetics*, *22*(20), 4127–4135. https://doi.org/10.1093/hmg/ddt261

Kramer, M. F. (2011). Stem-loop RT-qPCR for miRNAs. *Current Protocols in Molecular Biology*, Chapter 15. *95*(1). https://doi.org/10.1002/0471142727.mb1510s95

Lagier-Tourenne, C., Polymenidou, M., & Cleveland, D. W. (2010). TDP-43 and FUS/TLS: Emerging roles in RNA processing and neurodegeneration. *Human Molecular Genetics*, *19*(R1), R46–R64. https://doi.org/10.1093/hmg/ddq137

Lee, K. S., Kim, J., Kwak, S. N., Lee, K. S., Lee, D. K., Ha, K. S., Won, M. H., Jeoung, D., Lee, H., Kwon, Y. G., & Kim, Y. M. (2014). Functional role of NF-κB in expression of human endothelial nitric oxide synthase. *Biochemical and Biophysical Research Communications*, *448*(1), 101–107. https://doi.org/10.1016/j.bbrc.2014.04.079

Le Gall, L., Anakor, E., Connolly, O., Vijayakumar, U. G., Duddy, W. J., & Duguez, S. (2020). Molecular and cellular mechanisms affected in ALS. *Journal of Personalized Medicine*, *10*(3), 1–34. https://doi.org/10.3390/jpm10030101

Liddelow, S. A., & Barres, B. A. (2017). Reactive astrocytes: Production, function, and therapeutic potential. *Immunity*, *46*(6), 957–967. https://doi.org/10.1016/j.immuni.2017.06.006

Lopez-Verrilli, M. A., Picou, F., & Court, F. A. (2013). Schwann cell-derived exosomes enhance axonal regeneration in the peripheral nervous system. *Glia*, *61*(11), 1795–1806. https://doi.org/10.1002/glia.22558

Madill, M., McDonagh, K., Ma, J., Vajda, A., McLoughlin, P., O'Brien, T., Hardiman, O., & Shen, S. (2017). Amyotrophic lateral sclerosis patient iPSC-derived astrocytes impair autophagy via non-cell autonomous mechanisms. *Molecular Brain*, *10*(1), 942–954. https://doi.org/10.1186/s13041-017-0300-4

Marchetto, M. C. N., Muotri, A. R., Mu, Y., Smith, A. M., Cezar, G. G., & Gage, F. H. (2008). Non-cell-autonomous effect of human SOD1G37R astrocytes on motor neurons derived from human embryonic stem cells. *Cell Stem Cell*, *3*(6), 649–657. https://doi.org/10.1016/j.stem.2008.10.001

Marcuzzo, S., Bonanno, S., Kapetis, D., Barzago, C., Cavalcante, P., D'Alessandro, S., Mantegazza, R., & Bernasconi, P. (2015). Up-regulation of neural and cell cycle-related microRNAs in brain of amyotrophic lateral sclerosis mice at late disease stage. *Molecular Brain*, *8*(1), 661–674. https://doi.org/10.1186/s13041-015-0095-0

Marcuzzo, S., Kapetis, D., Mantegazza, R., Baggi, F., Bonanno, S., Barzago, C., Cavalcante, P., Kerlero de Rosbo, N., & Bernasconi, P. (2014). Altered miRNA expression is associated with neuronal fate in G93A-SOD1 ependymal stem progenitor cells. *Experimental Neurology*, *253*, 91–101. https://doi.org/10.1016/j.expneurol.2013.12.007

Massenzio, F., Peña-Altamira, E., Petralla, S., Virgili, M., Zuccheri, G., Miti, A., Polazzi, E., Mengoni, I., Piffaretti, D., & Monti, B. (2018). Microglial overexpression of fALS-linked mutant SOD1 induces SOD1 processing impairment, activation and neurotoxicity and is counteracted by the autophagy inducer trehalose. *Biochimica et Biophysica Acta, Molecular Basis of Disease*, *1864*(12), 3771–3785. https://doi.org/10.1016/j.bbadis.2018.10.013

Mishra, V., et al. (2020). Systematic elucidation of neuron-astrocyte interaction in models of amyotrophic lateral sclerosis using multi-modal integrated bioinformatics workflow. *Nature Communications*, *11*(1). https://doi.org/10.1038/S41467-020-19177-Y

Morel, L., Regan, M., Higashimori, H., Ng, S. K., Esau, C., Vidensky, S., Rothstein, J., & Yang, Y. (2013). Neuronal exosomal miRNA-dependent translational regulation of astroglial glutamate transporter GLT1. *Journal of Biological Chemistry*, *288*(10), 7105–7116. https://doi.org/10.1074/jbc.M112.410944

Murakami, A., Kojima, K., Ohya, K., Imamura, K., & Takasaki, Y. (2002). A new conformational epitope generated by the binding of recombinant 70-kD protein and U1 RNA to anti-U1 RNP autoantibodies in sera from patients with mixed connective tissue disease. *Arthritis and Rheumatism*, *46*(12), 3273–3282. https://doi.org/10.1002/art.10677

Nagai, M., Re, D. B., Nagata, T., Chalazonitis, A., Jessell, T. M., Wichterle, H., & Przedborski, S. (2007). Astrocytes expressing ALS-linked mutated SOD1 release factors selectively toxic to motor neurons. *Nature Neuroscience*, *10*(5), 615–622. https://doi.org/10.1038/nn1876

Nonaka, T., Masuda-Suzukake, M., Arai, T., Hasegawa, Y., Akatsu, H., Obi, T., Yoshida, M., Murayama, S., Mann, D. M. A., Akiyama, H., & Hasegawa, M. (2013). Prion-like properties of pathological TDP-43 aggregates from diseased brains. *Cell Reports*, *4*(1), 124–134. https://doi.org/10.1016/j.celrep.2013.06.007

Paez-Colasante, X., Figueroa-Romero, C., Sakowski, S. A., Goutman, S. A., & Feldman, E. L. (2015). Amyotrophic lateral sclerosis: Mechanisms and therapeutics in the epigenomic era. *Nature Reviews. Neurology*, *11*(5), 266–279. https://doi.org/10.1038/nrneurol.2015.57

Palacios, F., Cota, G., Horjales, S., Lima, A., Battistoni, J., Sotelo-Silveira, J., & Marín, M. (2010). An antibody-based affinity chromatography tool to assess Cu, Zn superoxide dismutase (SOD) G93A structural complexity in vivo. *Biotechnology Journal*, *5*(3), 328–334. http://dx.doi.org/10.1002/biot.200900106

Paraskevopoulou, M. D., Georgakilas, G., Kostoulas, N., Vlachos, I. S., Vergoulis, T., Reczko, M., Filippidis, C., Dalamagas, T., & Hatzigeorgiou, A. G. (2013). DIANA-microT web server v5.0: Service integration into miRNA functional analysis workflows. *Nucleic Acids Research*, *41*(Web Server issue), W169–W173. https://doi.org/10.1093/nar/gkt393

Park, H., & Poo, M. (2013). Neurotrophin regulation of neural circuit development and function. *Nature Reviews Neuroscience*, *14*(1), 7–23. http://dx.doi.org/10.1038/nrn3379

Pehar, M., Cassina, P., Vargas, M. R., Castellanos, R., Viera, L., Beckman, J. S., Estévez, A. G., & Barbeito, L. (2004). Astrocytic production of nerve growth factor in motor neuron apoptosis: Implications for amyotrophic lateral sclerosis. *Journal of Neurochemistry*, *89*(2), 464–473. https://doi.org/10.1111/j.1471-4159.2004.02357.x

Pehar, M., Harlan, B. A., Killoy, K. M., & Vargas, M. R. (2017). Role and therapeutic potential of astrocytes in amyotrophic lateral sclerosis. *Current Pharmaceutical Design*, *23*(33), 5010–5021. https://doi.org/10.2174/1381612823666170622095802

Perlson, E., Jeong, G. B., Ross, J. L., Dixit, R., Wallace, K. E., Kalb, R. G., & Holzbaur, E. L. F. (2009). A switch in retrograde signaling from survival to stress in rapid-onset neurodegeneration.

Journal of Neuroscience, *29*(31), 9903–9917. https://doi.org/10.1523/JNEUROSCI.0813-09.2009

Proia, P., Schiera, G., Mineo, M., Ingrassia, A. M. R., Santoro, G., Savettieri, G., & Di Liegro, I. (2008). Astrocytes shed extracellular vesicles that contain fibroblast growth factor-2 and vascular endothelial growth factor. *International Journal of Molecular Medicine*, *21*(1), 63–67. https://doi.org/10.3892/ijmm.21.1.63

Qin, J.-z., Wang, S.-j., & Xia, C. (2018). MicroRNAs regulate nitric oxide release from endothelial cells by targeting NOS3. *Journal of Thrombosis and Thrombolysis*, *46*(3), 275–282. https://doi.org/10.1007/s11239-018-1684-4

Raposo, G., & Stoorvogel, W. (2013). Extracellular vesicles: Exosomes, microvesicles, and friends. *Journal of Cell Biology*, *200*(4), 373–383. https://doi.org/10.1083/jcb.201211138

Ratajczak, J., Miekus, K., Kucia, M., Zhang, J., Reca, R., Dvorak, P., & Ratajczak, M. Z. (2006). Embryonic stem cell-derived microvesicles reprogram hematopoietic progenitors: Evidence for horizontal transfer of mRNA and protein delivery. *Leukemia*, *20*(5), 847–856. https://doi.org/10.1038/sj.leu.2404132

Record, M., Carayon, K., Poirot, M., & Silvente-Poirot, S. (2014). Exosomes as new vesicular lipid transporters involved in cell–cell communication and various pathophysiologies. *Biochimica et Biophysica Acta (BBA) - Molecular and Cell Biology of Lipids*, *1841*(1), 108–120. https://doi.org/10.1016/j.bbalip.2013.10.004

Rotem, N., Magen, I., Ionescu, A., Gershoni-Emek, N., Altman, T., Costa, C. J., Gradus, T., Pasmanik-Chor, M., Willis, D. E., Ben-Dov, I. Z., Hornstein, E., & Perlson, E. (2017). ALS along the axons - Expression of coding and noncoding RNA differs in axons of ALS models. *Scientific Reports*, *7*(1), 44500. https://doi.org/10.1038/srep44500

Russell, A. P., Wada, S., Vergani, L., Hock, M. B., Lamon, S., Léger, B., Ushida, T., Cartoni, R., Wadley, G. D., Hespel, P., Kralli, A., Soraru, G., Angelini, C., & Akimoto, T. (2013). Disruption of skeletal muscle mitochondrial network genes and miRNAs in amyotrophic lateral sclerosis. *Neurobiology of Disease*, *49*(1), 107–117. https://doi.org/10.1016/j.nbd.2012.08.015

Saucier, D., Wajnberg, G., Roy, J., Beauregard, A. P., Chacko, S., Crapoulet, N., Fournier, S., Ghosh, A., Lewis, S. M., Marrero, A., O'Connell, C., Ouellette, R. J., & Morin, P. (2019). Identification of a circulating miRNA signature in extracellular vesicles collected from amyotrophic lateral sclerosis patients. *Brain Research*, *1708*, 100–108. https://doi.org/10.1016/j.brainres.2018.12.016

Sbai, O., Ould-Yahoui, A., Ferhat, L., Gueye, Y., Bernard, A., Charrat, E., Mehanna, A., Risso, J.-J., Chauvin, J.-P., Fenouillet, E., Rivera, S., & Khrestchatisky, M. (2010). Differential vesicular distribution and trafficking of MMP-2, MMP-9, and their inhibitors in astrocytes. *Glia*, *58*(3), 344–366. https://doi.org/10.1002/glia.20927

Sherman, B. T., Hao, M., Qiu, J., Jiao, X., Baseler, M. W., Lane, H. C., Imamichi, T., & Chang, W. (2022). DAVID: a web server for functional enrichment analysis and functional annotation of gene lists (2021 update). *Nucleic Acids Research*, *50*(W1), W216–W221. https://doi.org/10.1093/nar/gkac194

Shi, R., Wang, P. Y., Li, X. Y., Chen, J. X., Li, Y., Zhang, X. Z., Zhang, C. G., Jiang, T., Li, W.-B., Ding, W., & Cheng, S. J. (2015). Exosomal levels of miRNA-21 from cerebrospinal fluids associated with poor prognosis and tumor recurrence of glioma patients. *Oncotarget*, *6*(29), 26971–26981. https://doi.org/10.18632/oncotarget.4699

Silverman, J. M., Christy, D., Shyu, C. C., Moon, K.-M., Fernando, S., Gidden, Z., Cowan, C. M., Ban, Y., Stacey, R. G., Grad, L. I., McAlary, L., Mackenzie, I. R., Foster, L. J., & Cashman, N. R. (2019). CNS-derived extracellular vesicles from superoxide dismutase 1 (SOD1)G93A ALS mice originate from astrocytes and neurons and carry misfolded SOD1. *Journal of Biological Chemistry*, *294*(10), 3744–3759. https://doi.org/10.1074/jbc.RA118.004825

Tarassishin, L., Loudig, O., Bauman, A., Shafit-Zagardo, B., Suh, H. S., & Lee, S. C. (2011). Interferon regulatory factor 3 inhibits astrocyte inflammatory gene expression through suppression of the proinflammatory miR-155 and miR-155. *Glia*, *59*(12), 1911–1922. https://doi.org/10.1002/glia.21233

Taylor, A. R., Robinson, M. B., Gifondorwa, D. J., Tytell, M., & Milligan, C. E. (2007). Regulation of heat shock protein 70 release in astrocytes: Role of signaling kinases. *Developmental Neurobiology*, *67*(13), 1815–1829. https://doi.org/10.1002/dneu.20559

Thery, C., et al. (1999). Molecular characterization of dendritic cell-derived exosomes. Selective accumulation of the heat shock protein hsc73. *Journal of Cell Biology*, *147*(3), 599–610. https://doi.org/10.1083/jcb.147.3.599

Valadi, H., Ekström, K., Bossios, A., Sjöstrand, M., Lee, J. J., & Lötvall, J. O. (2007). Exosome-mediated transfer of mRNAs and microRNAs is a novel mechanism of genetic exchange between cells. *Nature Cell Biology*, *9*(6), 654–659. https://doi.org/10.1038/ncb1596

Van Harten, A. C. M., Phatnani, H., & Przedborski, S. (2021). Non-cell-autonomous pathogenic mechanisms in amyotrophic lateral sclerosis. *Trends in Neurosciences*, *44*(8), 658–668. https://doi.org/10.1016/j.tins.2021.04.008

Varcianna, A., Myszczynska, M. A., Castelli, L. M., O'Neill, B., Kim, Y., Talbot, J., Nyberg, S., Nyamali, I., Heath, P. R., Stopford, M. J., Hautbergue, G. M., & Ferraiuolo, L. (2019). Micro-RNAs secreted through astrocyte-derived extracellular vesicles cause neuronal network degeneration in C9orf72 ALS. *EBioMedicine*, *40*, 626–635. https://doi.org/10.1016/j.ebiom.2018.11.067

Vargas, M. R., Pehar, M., Cassina, P., Beckman, J. S., & Barbeito, L. (2006). Increased glutathione biosynthesis by Nrf2 activation in astrocytes prevents p75NTR-dependent motor neuron apoptosis. *Journal of Neurochemistry*, *97*(3), 687–696. https://doi.org/10.1111/j.1471-4159.2006.03742.x

Vargas, M. R., Pehar, M., Cassina, P., Estévez, A. G., Beckman, J. S., & Barbeito, L. (2004). Stimulation of nerve growth factor expression in astrocytes by peroxynitrite. *In Vivo*, *18*(3), 269–274.

Vaz, A. R., Pinto, S., Ezequiel, C., Cunha, C., Carvalho, L. A., Moreira, R., & Brites, D. (2019). Phenotypic effects of wild-type and mutant SOD1 expression in N9 murine microglia at steady state, inflammatory and immunomodulatory conditions. *Frontiers in Cellular Neuroscience*, *13*, 505–520. https://doi.org/10.3389/FNCEL.2019.00109

Verkhratsky, A., Ho, M. S., Zorec, R., & Parpura, V. (2019). The concept of neuroglia. In *Advances in experimental medicine and biology* (pp. 1–13). Springer New York LLC.

Vlachos, I. S., Paraskevopoulou, M. D., Karagkouni, D., Georgakilas, G., Vergoulis, T., Kanellos, I., Anastasopoulos,

I. L., Maniou, S., Karathanou, K., Kalfakakou, D., Fevgas, A., Dalamagas, T., & Hatzigeorgiou, A. G. (2015). DIANA-TarBase v7.0: Indexing more than half a million experimentally supported miRNA:MRNA interactions. *Nucleic Acids Research*, *43*(Database issue), D153–D159. https://doi.org/10.1093/nar/gku1215

Wang, L., Gutmann, D. H., & Roos, R. P. (2011a). Astrocyte loss of mutant SOD1 delays ALS disease onset and progression in G85R transgenic mice. *Human Molecular Genetics*, *20*(2), 286–293. https://doi.org/10.1093/hmg/ddq463

Wang, L., Sharma, K., Grisotti, G., & Roos, R. P. (2009). The effect of mutant SOD1 dismutase activity on non-cell autonomous degeneration in familial amyotrophic lateral sclerosis. *Neurobiology of Disease*, *35*(2), 234–240. https://doi.org/10.1016/j.nbd.2009.05.002

Wang, S., Cesca, F., Loers, G., Schweizer, M., Buck, F., Benfenati, F., Schachner, M., & Kleene, R. (2011b). Synapsin I is an oligomannose-carrying glycoprotein, acts as an oligomannose-binding lectin, and promotes neurite outgrowth and neuronal survival when released via glia-derived exosomes. *Journal of Neuroscience*, *31*(20), 7275–7290. https://doi.org/10.1523/JNEUROSCI.6476-10.2011

Westergard, T., Jensen, B. K., Wen, X., Cai, J., Kropf, E., Iacovitti, L., Pasinelli, P., & Trotti, D. (2016). Cell-to-cell transmission of dipeptide repeat proteins linked to C9orf72-ALS/FTD. *Cell Reports*, *17*(3), 645–652. https://doi.org/10.1016/j.celrep.2016.09.032

Yamanaka, K., Boillee, S., Roberts, E. A., Garcia, M. L., McAlonis-Downes, M., Mikse, O. R., Cleveland, D. W., & Goldstein, L. S. B. (2008a). Mutant SOD1 in cell types other than motor neurons and oligodendrocytes accelerates onset of disease in ALS mice. *Proceedings of the National Academy of Sciences of the United States of America*, *105*(21), 7594–7599. https://doi.org/10.1073/pnas.0802556105

Yamanaka, K., Chun, S. J., Boillee, S., Fujimori-Tonou, N., Yamashita, H., Gutmann, D. H., Takahashi, R., Misawa, H., & Cleveland, D. W. (2008b). Astrocytes as determinants of disease progression in inherited amyotrophic lateral sclerosis. *Nature Neuroscience*, *11*(3), 251–253. https://doi.org/10.1038/nn2047

Yu, Z., Liu, H., Fan, J., Chen, F., & Liu, W. (2020). MicroRNA-155 participates in the expression of LSD1 and proinflammatory cytokines in rheumatoid synovial cells. *Mediators of Inflammation*, *2020*, 1–11. https://doi.org/10.1155/2020/4092762

Zhang, J., Li, S., Li, L., Li, M., Guo, C., Yao, J., & Mi, S. (2015). Exosome and exosomal microRNA: Trafficking, sorting, and function. *Genomics, Proteomics & Bioinformatics*, *13*(1), 17–24. https://doi.org/10.1016/j.gpb.2015.02.001

Zhang, Z., Almeida, S., Lu, Y., Nishimura, A. L., Peng, L., Sun, D., Wu, B., Karydas, A. M., Tartaglia, M. C., Fong, J. C., Miller, B. L., Farese, R. V., Moore, M. J., Shaw, C. E., & Gao, F. B. (2013). Downregulation of microRNA-9 in iPSC-derived neurons of FTD/ALS patients with TDP-43 mutations. *PLoS One*, *8*(10), e76055. https://doi.org/10.1371/journal.pone.0076055

Zhou, F., Guan, Y., Chen, Y., Zhang, C., Yu, L., Gao, H., Du, H., Liu, B., & Wang, X. (2013). miRNA-9 expression is upregulated in the spinal cord of G93A-SOD1 transgenic mice. *International Journal of Clinical and Experimental Pathology*, *6*(9), 1826–1838.